ABSTRACT

ANTONIK, MARGARET. Performance and Design Comparison of a Bulk Thermoelectric Cooler with a Hybrid Device Architecture. (Under the direction of Dr. Scott Ferguson).

This thesis compares the economic viability and performance outcomes of two different thermoelectric device architectures to determine the advantages and appropriate use of each configuration. Hybrid thermoelectric coolers employ thin-film thermoelectric materials sandwiched between a plastic substrate and formed into a corrugated structure. Roll-to-roll manufacturing and low-cost polymer materials offer a cost advantage to the hybrid architecture at the sacrifice of performance capabilities while conventional bulk devices offer increased performance at a higher cost. Performance characteristics and cost information are developed for both hybrid and conventional bulk single-stage thermoelectric modules. The design variables include device geometry, electrical current input, and thermoelectric material type. The trade-offs between cooling performance and cost will be explored and the thermoelectric system configuration analyzed for both hybrid and conventional bulk thermoelectric coolers.

Performance and Design Comparison of a Bulk Thermoelectric Cooler with a Hybrid Device Architecture

by
Margaret Antonik

A thesis submitted to the Graduate Faculty of
North Carolina State University
in partial fulfillment of the
requirements for the degree of
Master of Science

Mechanical Engineering

Raleigh, North Carolina

2015

APPROVED BY:

_____
Dr. Scott Ferguson
Committee Chair

_____ _____
Dr. Brendan O'Connor Dr. Stephen Terry

BIOGRAPHY

Margaret Antonik was born and raised in Central Florida, where family, sports, especially soccer, and academics were integral parts of her life. With the desire to play Division I soccer at an academically challenging university, Margaret moved north to South Carolina to earn a degree in mathematics at Furman University while playing on the women's soccer team. After three years of working in various jobs and developing hobbies that piqued an interest in engineering, she decided to pursue a master's degree in mechanical engineering and to attend North Carolina State University.

TABLE OF CONTENTS

LIST OF TABLES

LIST OF FIGURES

LIST OF NOMENCLATURE

A	Cross-sectional area
C	Cost
$C``$	Areal material cost
$C```$	Volumetric material cost
COP	Coefficient of Performance
d_s	Substrate thickness
I	Input current
K	Thermal conductivity
L	TE leg length
N	Number of thermocouples
P	Input power
Q	Cooling/heating capacity
R	Electrical conductivity
r	Amortization rate
T	Absolute temperature
t	TE leg thickness
U	Heat exchanger overall heat transfer coefficient
w	TE leg width
ZT	Thermoelectric material figure of merit

Greek Symbols

α	Seebeck coefficient
κ	Thermal conductivity
ρ	Electrical resistivity
ψ	Dimensionless spreading resistance

Subscripts

C	Cold side
H	Hot side
HX	Heat exchanger
n	n-type material
p	p-type material
s	substrate
TE	Thermoelectric material

1. INTRODUCTION

Increased interest in sustainable practices and environmentally friendly products has driven the exploration of green technologies. During industrial processes, twenty to fifty percent of energy consumed is lost to waste heat, and approximately sixty percent of this waste heat is under 450°F and considered low quality [1]. By capturing waste heat and taking advantage of natural temperature differences, thermoelectric generators (TEGs) offer the potential to be an important source of clean and renewable energy. According to the Environmental Protection Agency, a given mass of the commonly used R-134a refrigerant contributes 1,300 times more to global warming over a given time period than the same mass of carbon dioxide [2]. In contrast to conventional refrigeration and air conditioning, thermoelectric coolers (TECs) might be a viable alternative to traditional systems that employ potentially harmful refrigerants. While the advantages of thermoelectric technology are promising, a major drawback preventing widespread adoption is their inefficiency. To work beyond niche applications of TECs, this thesis explores the optimization of a thermoelectric device architecture that may overcome this limitation and allow thermoelectric devices to be designed that fully exploit their potential.

1.1. Overview of Thermoelectrics

Thermoelectric (TE) modules are quiet, reliable, and scalable solid-state devices that use TE materials to 1) convert waste heat to energy via the Seebeck effect or 2) convert energy to cooling or heating via the Peltier effect. Discovered in 1821, the Seebeck effect is what drives TEGs [3]. Thomas Johann Seebeck demonstrated that heating the junction between two connected, dissimilar wires (called a thermocouple) created a small voltage on a

voltmeter attached to the other end of the wires. J. Peltier demonstrated the Peltier effect thirteen years later by showing that an electric current passing through the wires created heating or cooling depending on the direction of the current flow. William Thomson observed a third thermoelectric phenomenon that explains the relationship between the Peltier and Seebeck effects. The Thomson effect describes reversible heating and cooling when there is both current flow through the device and temperature differential across the device [4].

Modern semiconductor materials tailored towards thermoelectric applications allow TE devices to more efficiently demonstrate the Peltier and Seebeck effects. Free electrons or holes flow through connected p-type (current carried by mobile holes) and n-type (current carried by mobile electrons) semiconductors. As heat is applied to a device, electrons and holes flow from one side of the device to the other side, creating a voltage difference and driving the Seebeck effect. As given in Eq. (1.1), the Seebeck coefficient (α) describes the relationship between a given temperature difference across a device (designated by temperature T_H on the hot side of the device and T_C on the cold side) and the corresponding voltage difference (V).

$$V = \alpha(T_H - T_C) \tag{1.1}$$

As current passes through the semiconductor pairs of a TEC, holes and electrons gather on one side of the device, carrying heat away from the junction where they are connected. That side of the module then becomes cold. The Peltier coefficient (π), given in Eq. (1.2), describes the heat flow produced (Q) per unit of electric current (I).

$$\pi = \frac{Q}{I} \tag{1.2}$$

Figure 1.1 depicts a simple, single thermocouple for a TEG (a) and TEC (b) consisting of a pair of n-type and p-type semiconductors and the current flow and heat flow through the device.

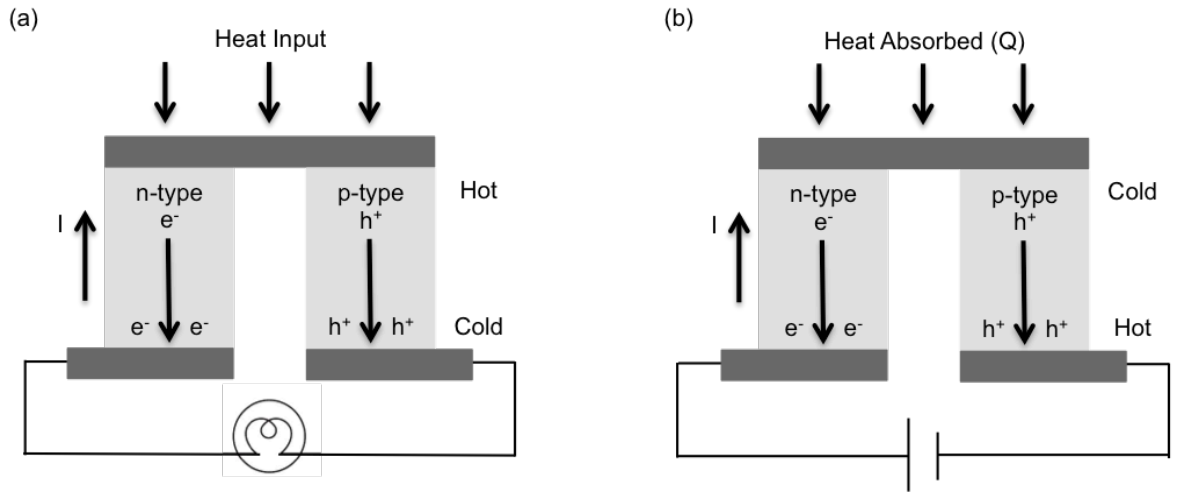

Figure 1.1 Diagram of (a) Seebeck Effect in a Thermoelectric Generator and (b) Peltier Effect in a Thermoelectric Cooler

In the 1990s, advances in the theory and concepts of electron and phonon transport in TE materials led to a renewed focus on thermoelectrics as a green technology [5]. Nanostructured and complex bulk materials allow for thermoelectric materials with improved efficiencies to compete with other energy generating or cooling technologies [6]. *ZT*, given in Eq. (1.3), is the figure of merit measuring the efficiency of a thermoelectric material. Furthermore, a material's *ZT* value directly relates to the overall efficiency of a device. A

function of absolute temperature (T), maximizing ZT requires a large Seebeck coefficient (α), low thermal conductivity (κ), and low electrical resistivity (ρ). ZT is given by Eq. (1.3).

$$ZT = \frac{\alpha^2}{\kappa\rho}T \tag{1.3}$$

1.2. Motivation

The focus of this work is on TECs as TEGs have been more widely explored for their performance limits and cost advantages. Additionally, TECs have several advantages, such as their solid-state nature with no working fluids, that make TE technology a desirable alternative over traditional refrigeration and cooling methods. Eliminating the need for ozone-depleting hydrochlorofluorocarbon (HCFC) and greenhouse-gas emitting (due to leaks, service losses, and disposal) hydrofluorcarbon (HFC) refrigerants, TECs are an environmentally friendly alternative. Additionally, TECs can be used in a variety of applications where durability and reliability are paramount considerations. The industry standard for mean time between failures (MTBF) is over 200,000 hours while a traditional chiller has an MTBF of approximately 18,000 to 82,000 hours [7].

Diverse applications of TECs that are currently being explored include commercial products, military purposes, aerospace uses, scientific and medical equipment, microelectronics, and solar-driven thermoelectric cooling devices [8]. Climate-control seat systems constructed with TEC technology can reduce fuel consumption in hybrid vehicles [9]. TECs used in microprocessor cooling systems offer an efficient and cost-effective way of controlling chip temperatures [9], [10]. Solar-driven thermoelectric coolers and heaters are being investigated as heat pumps where the source of electrical power eliminates fossil fuel

power usage [11]. Historically, however, TE devices have not met the efficiency capabilities of current energy conversion or cooling technologies to reach widespread adoption.

A major drawback of TECs is their inefficiency. Typical *ZT* values of thermoelectric materials, including the widely used bismuth-telluride (BiTe) semiconductors, on the market are around 1 [9]. Assuming a *ZT* value of 1, the efficiency of a TEC is only 10-15% of Carnot efficiency, whereas vapor compression cooling is at 60% of Carnot. If average *ZT* values were greater than 2, thermoelectric heating, ventilating, and cooling systems could become attractive alternatives to traditional systems [9]. The low efficiency of the material directly translates into low efficiency of the overall device, as measured by the Coefficient of Performance (*COP*). *COP* is a common metric used to measure the efficiency of any heat pump.

Figure 1.2 demonstrates the differences between *COP*s of different cooling technologies. The Carnot Cycle on this figure represents the ideal *COP* where the heat pump is operating at maximum theoretical efficiency. Important to note is the efficiency of traditional household vapor-compression refrigerators and air conditioners at *COP*s ranging between 2 and 4. In contrast, a typical *COP* of TECs is below the threshold established by these traditional cooling methods except when the *ZT* value is increased or when the system is operating at very low temperature differentials.

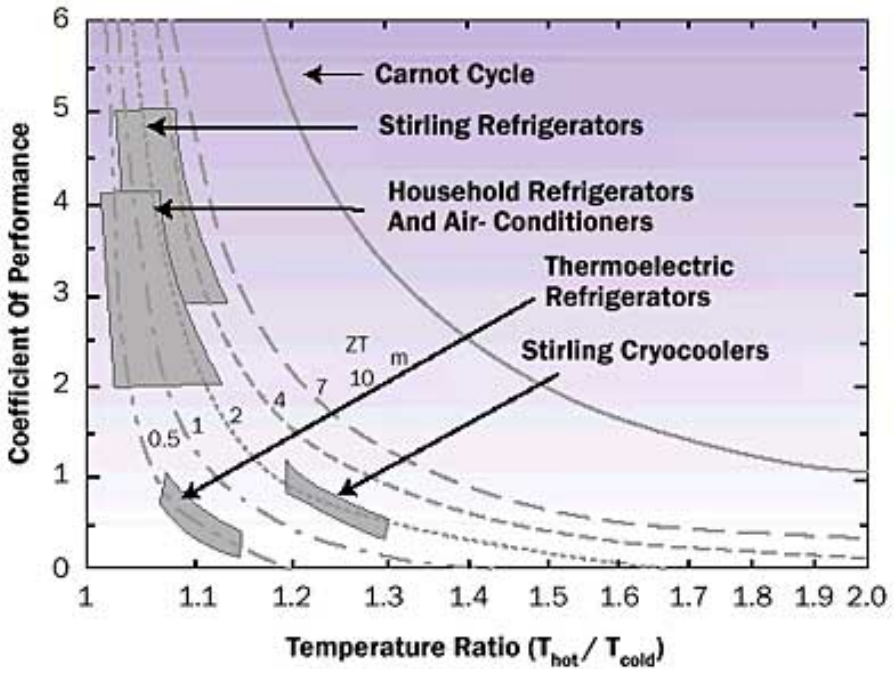

Figure 1.2. Comparison of the Coefficient of Performance of Cooling Technologies [12]

While presenting a trade-off in performance, low-cost and large-scale manufacturing of TE devices may provide an alternative to the conventional, difficult to manufacture bulk devices. The TE materials currently available for large-scale processing are less efficient than BiTe material commonly used in bulk processing. In addition, novel architectures are needed to maintain a heat flow across a device similar to how a bulk device operates—this allows for easier maintenance of a temperature differential across a device. However, introducing a low cost alternative may make the sacrifice of TEC efficiency acceptable. Environmentally friendly and stable polymer TE materials offer a printable solution that can be used in R2R (Roll-to-Roll) manufacturing on flexible substrates. In comparison to current inorganic materials like BiTe, the best reported *ZT* value for polymer TE material poly(3,4-

ethylenedioxythiophene) (PEDOT) is 0.25 [13]. Ongoing research is exploring the screen printing of PEDOT in a R2R manufacturing process to produce thin-film TE devices [14].

TECs have the potential for widespread use, but a better understanding of the performance and design space is needed to drive future development. Despite recent advancements in material efficiency, additional improvements must be weighed against the added overall system costs. Geometry of the device, power input into the cooler, operating parameters, and the heat exchanger characteristics are contributing factors to the efficiency of a TEC. Additionally, the exploration of different device architectures may allow for higher performing, lower cost TECs.

Along with an analysis on device geometry, material choice, and input current, this work explores a hybrid architecture that combines a conventional bulk device with an in-plane thin film device. A bulk device has TE material deposited on a substrate in thicknesses on the order of millimeters; in contrast, thin-film deposits on the substrate are microns thick. This leads to a challenge of maintaining a temperature differential across the device. While taking advantage of low-cost R2R manufacturing to print thin-film layers of TE material on a substrate, the hybrid architecture is able to maintain a cross-plane heat flux like in a bulk device, allowing for improved maintenance of a temperature differential across the device. Analysis is needed that goes beyond the scope of just studying thermoelectric materials and their efficiency to develop cost-effective, high performing TECs. The geometric factors, heat exchanger options, device architecture, TE material, and operating current all play a large role in not only the cooling performance and efficiency of a TEC but also the overall system costs.

1.3. Research Goals

As mentioned previously, the focus of this work is on TECs as TEGs have been more widely explored for their performance limits and cost advantages. To enable wider applications of TECs, two main research questions will be addressed. The first question relates to the use of design optimization to gain insights into the performance space and design space of an overall TEC system:

Research question 1: What insights into the design and performance spaces of a thermoelectric cooler can be realized when using optimization and a new cost metric?

Toward this goal, this study extends an existing cost metric and expands the performance equations for TEC analysis [3], [15]–[17]. Additional performance considerations include a heat exchanger and spreading resistance. Unlike previous analysis of TECs, this study considers multiple objectives, additional design variables and model considerations, a heat exchanger on the hot side of the TEC, and multiple TE materials. Furthermore, both bulk and hybrid device architectures are compared. Exploring the economic and performance characteristics of a TEC manufactured via screen-printing techniques offers insights into the viability of roll-to-roll manufacturing's applicability to TE devices.

The second research question directly follows the first:

Research question 2: How do improvements in the thermoelectric material figure of merit and a better understanding of the major cost components impact the performance outcomes of a thermoelectric cooler?

The goal of this question is to demonstrate how insights gained from design optimization may allow for expanded use of TECs. TECs have the potential for widespread use, but a better understanding of the performance and design space is needed to drive future development. Despite recent advancements in the efficiency of the materials, additional improvements must be made for TECs to be competitive with traditional methods of refrigeration [9]. To work towards this goal, materials with improved thermoelectric figures of merit will be explored, and system costs will be decomposed to identify major contributions to the overall cost of a TEC. Through identification of heat exchanger, substrate, and TE material costs as well as the impact of increased TE material efficiency, a more complete understanding of the potential for TECs to reach wider adoption is realized. By addressing these two research questions, this work will add to the overall body of research on TECs and highlight potential device architectures capable of bridging the gap between theoretical analysis and practical application.

1.4. Thesis Outline

To provide more detailed motivation for this work and context for the topics covered in this thesis, Chapter 2 provides a background on thermoelectric materials, device architectures, roll-to-roll manufacturing, and previous work in design optimization. Chapter 3 presents the analytical model of a TEC, including the additional design considerations of the heat exchanger and spreading resistance, and discusses how the new cost will be incorporated into this study. Chapter 4 presents the problem formulations used in the design optimization and introduces the algorithms used to solve for optimum solutions, and Chapter 5 follows with results of the design optimization and discussion pertinent to answering the two research

questions. Additionally, a simplified design scenario is presented to begin shifting from theoretical insights on TECs to design applications. This work concludes with Chapter 6 to summarize the results and detail areas of future work.

2. BACKGROUND

Thermoelectric coolers have been widely explored to maximize their efficiency and cooling capabilities, but analysis has focused on the development of more efficient thermoelectric materials, analysis of bulk and thin-film device architectures, and the optimization of the geometry factors of conventional TEC structures [9]. TE materials are an integral part of determining the efficiency of a device, and, as a result, improving TE materials and structuring semiconductor materials to suit TE applications is a primary research direction.

The differences between bulk and thin-film device architectures have also been studied, and researchers have introduced novel designs that blend the advantages of the bulk and thin-film devices [3], [18]–[20]. These novel designs, described further in section 2.2, introduce unique architectures and structures that enable the device to retain a cross-plane heat flux like a bulk device but utilize thin-film manufacturing methods that are automated and low-cost. Furthermore, R2R manufacturing has been introduced as an avenue towards large-scale, low-cost production of thin-film and novel TECs and TEGs [14], [21], [22] Lastly, design optimization studies aimed at improving the efficiency, minimizing costs, and maximizing performance of TE devices offer general insights into the design of a TE device. By studying certain components or design factors of TE devices instead of considering a total system, including heat exchangers, device geometries, and operating current, these studies have provided information regarding device geometry and two performance characteristics: cooling capacity (Q_C) and *COP*.

In [9], four research areas are identified to work towards higher efficiency TE devices: improve the *ZT* values of materials, use design optimization and reduce parasitic losses by using nontraditional materials, explore alternative thermodynamic cycles, and, lastly, consider unconventional device architectures. As an introduction to these research areas, the background section reviews the current advancements in TE materials, device architectures introduced in the literature, the R2R manufacturing process, and research on the design optimization of TE devices. The work introduced in this thesis builds upon the research discussed in the background section by incorporating additional design considerations, analyzing a novel TEC device architecture, and expanding a cost metric established in the literature to a TEC system to include the device and a heat exchanger. Additional design space parameters will be considered and the performance metrics used go beyond those discussed in the literature by accounting for cost, spreading resistance, and heat exchangers.

2.1. Thermoelectric Materials

A difficulty in advancing the efficiency of thermoelectric devices is the trade-off presented in developing higher performing materials. Conflicting goals to increase the Seebeck coefficient, decrease thermal conductivity, and increase electrical conductivity exist when improving the figure of merit of a material [3]. Each of these factors influencing the efficiency of materials is a function of charge carrier concentration. As the charge carrier concentration increases, both electrical conductivity and the Seebeck coefficient increase. Additionally, the thermal conductivity of the material also increases as the charge carrier concentration grows, introducing a thermal component to the electrical charge carrying

characteristics of the material. This electronic component of thermal conductivity typically accounts for 1/3 of the overall thermal conductivity of TE materials [3]. The heat conducted through the legs due to thermal conductivity limits the ability of a thermocouple to produce or maintain a temperature difference across the device, and a large electrical conductivity reduces the Joule heating in a device. In addition, these three properties are temperature dependent. These trade-offs observed when increasing the charge carrier concentration, depicted in Figure 2.1, represent the challenge in developing materials with large figures of merit to apply to TE applications.

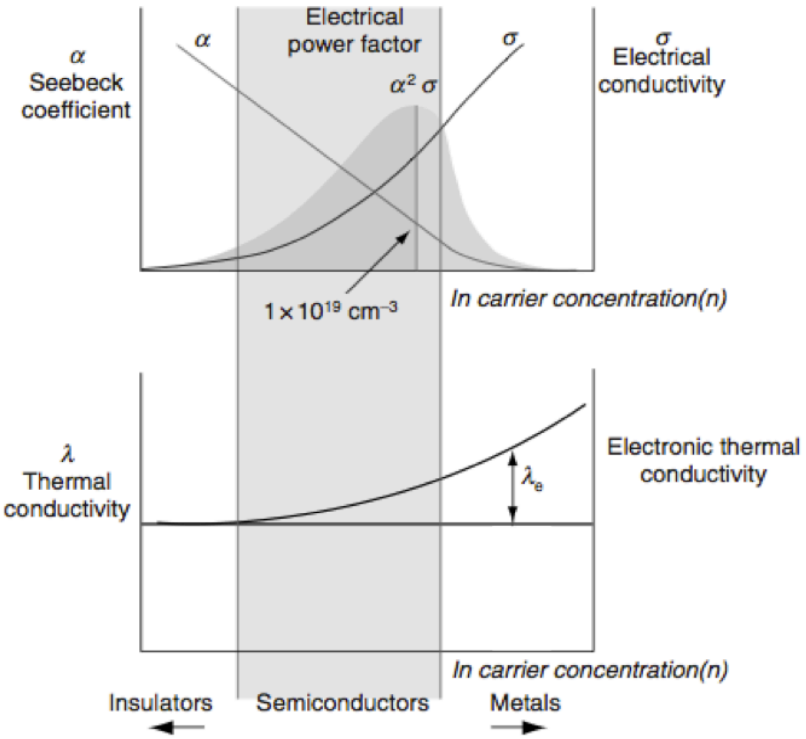

Figure 2.1. Dependence of Seebeck Coefficient (α), Electrical Conductivity (σ), and Thermal Conductivity (λ) on Charge Carrier Concentration, adapted from [3]

Researchers discovered in 1911 that a thermocouple's performance improved by increasing the Seebeck coefficient (demonstrated in Eq. (1.1), creating an improved voltage difference for a given difference in temperature), increasing the electrical conductivity, and decreasing the thermal conductivity [4]. Until semiconductors were introduced as thermoelectric materials in the 1950s, thermocouples that produced appreciable outputs of power or cooling were not realized [4]. Performance gains were an order of magnitude larger than previously used TE devices, and continued tuning of semiconductor doping techniques allowed for *ZT* values approaching 1. While metals have high electrical conductivities and insulators have low electrical conductivities, semiconductors have intermediate values, allowing for carrier concentrations suitable for optimized *ZT* values. Three basic groupings of TE materials were introduced: bismuth-based alloys (suitable for low temperatures up to 450 K), lead tellurium (suitable for mid-range temperature applications up to 850 K), and silicon-based alloys (suitable for temperatures up to 1300 K) [3]. Bismuth Telluride (Bi_2Te_3), with *ZT* values ranging from 0.8 to 1.1, has been the most common material used in commercial thermoelectric applications [6]. *ZT* values greater than 1 were made possible using semiconductors in TE applications. The advancements demonstrated the use of nanostructural engineering and complex cystal-structure bulk materials (including skutterides and clathrates) to develop high performing TE materials. In general, advances in material efficiency have occurred by suppressing any increase in thermal conductivity [6].

The complex cell structures of skutterides and clathrates, which are lattice shapes that trap molecules with low thermal conductivities, were introduced as a way to achieve high figures of merit [6]. By trapping molecules with low thermal conductivities, the TE

material's thermal conductivity is suppressed, and the material's *ZT* value can improve. Superlattice materials that alternate layers of semiconductors and increase the number of charge carrying electrons while inhibiting the number of heat carrying phonons showed promise in high-efficiency TE materials—a *ZT* value of 2.4 was reported for these thin-film superlattice materials [23]. The application of quantum dots, which are nanocrystal semiconductor structures, has also introduced materials with reported *ZT* values over 2. The evolution of these materials and their associated increases in *ZT* values is given in Figure 2.2.

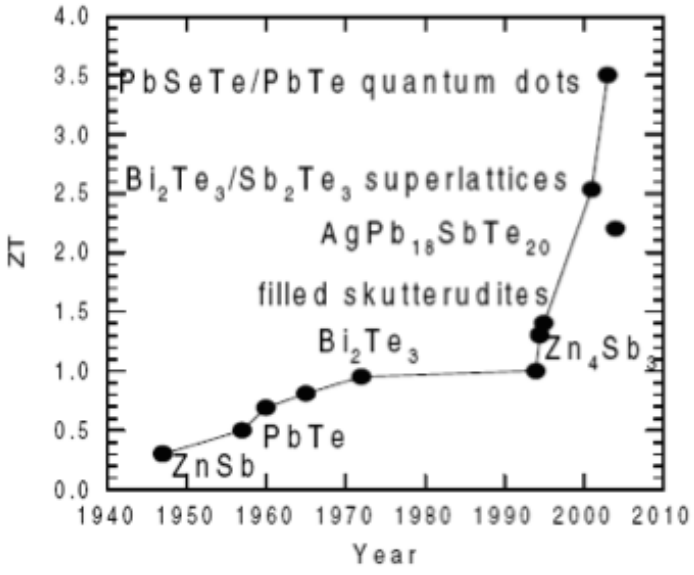

Figure 2.2. Evolution of Thermoelectric Material Advancements [24]

While these advancements in material efficiency have indicated that TE devices can be competitive alternatives to conventional cooling and energy generation techniques, the added costs and complexities must be considered. With these advancements in materials,

often an increase in cost and difficulty in scaling up production to large-scale manufacturing is introduced. LeBlanc et. al discuss the differences in manufacturing of these materials [15]. Superlattices use a complex fabrication process that requires hours to deposit a thin layer of material, driving the cost of production up and increasing the difficulty in manufacturing [15]. Other nanostructured materials offer only a small increase in manufacturing cost over conventional bulk materials, but both nanostructured and bulk materials are subject to expensive areal dicing and metallization manufacturing costs [15]. As a result of the manufacturing and processing difficulties of the aforementioned materials, researchers have identified easy-to-fabricate organic polymer materials as a possible TE material suitable for large-scale and low-cost production of TECs and TEGs. Polymers intrinsically have very low thermal conductivities—unlike advancements in the previously mentioned inorganic materials, improvements in the efficiency of polymers can be realized by increasing the Seebeck coefficient and electrical conductivity rather than just limiting increases in thermal conductivity. While the advantages of poly(3,4-ethylenedioxythiophene) (PEDOT) polymer materials are plenty, including the incorporation of printing techniques to replace specialized metallization and other manufacturing techniques, they are currently limited by their low Seebeck coefficient and electrical conductivity, but the research in this area is very recent [25]. As a result, the highest reported *ZT* value is only 0.25 [25].

While the nanoscale design of semiconductor TE materials is not a focus of this research, an understanding of how the thermoelectric materials work and the limitations of the materials is necessary to the formulation of the design optimization and analysis of different device architectures. Each of the materials discussed, from superlattices to

nanostructured materials to conventional BiTe to PEDOT, are incorporated into the design optimization problems discussed in this research. Improvements in material efficiency and increased *ZT* values are constantly advancing the applicability of TE devices in more uses. However, as mentioned previously, the advancement of material efficiency is only one aspect of realizing the potential of TE devices in more widespread applications. The next section will discuss the various device architectures seen throughout the literature and provide a context for how the TE materials are used in a device system.

2.2. Device Architectures

As discussed in this section, different device architectures have been explored to suit specific applications of cooling or energy generation with increased performance or reduced cost. For the purposes of this work, TEC device architectures are grouped into three categories: bulk, thin-film, and hybrid [3], [18], [26]. These architectures are typically differentiated by two different orientations of heat flux: cross-plane heat and current flow (perpendicular to the substrate) and in-plane heat and current flow (parallel to the substrate) relative to the surface of the device. Figure 2.3 depicts the differences between the types of architectures.

The most common TE device is a bulk module, as shown in Figure 2.3(a), consisting of Bi_2Te_3 legs (with lengths from a few hundred microns to a couple millimeters) connected by metal contacts and sandwiched between a ceramic substrate. Conventional, bulk TECs produce a cross-plane heat flow which allows for easier maintenance of the temperature difference (between the hot side and cold side) across the device. Thin-film devices (deposited with leg lengths under a few hundred microns) have in-plane heat flow across the

device as shown in Figure 2.3(b). Configurations that use the advantages of both thin-film properties and cross-plane heat flow are designated as hybrid architectures. Hybrid architectures take advantage of thin-film technology, alternative manufacturing techniques like printing, and their small size while maintaining a temperature differential across the device using cross-plane heat flux.

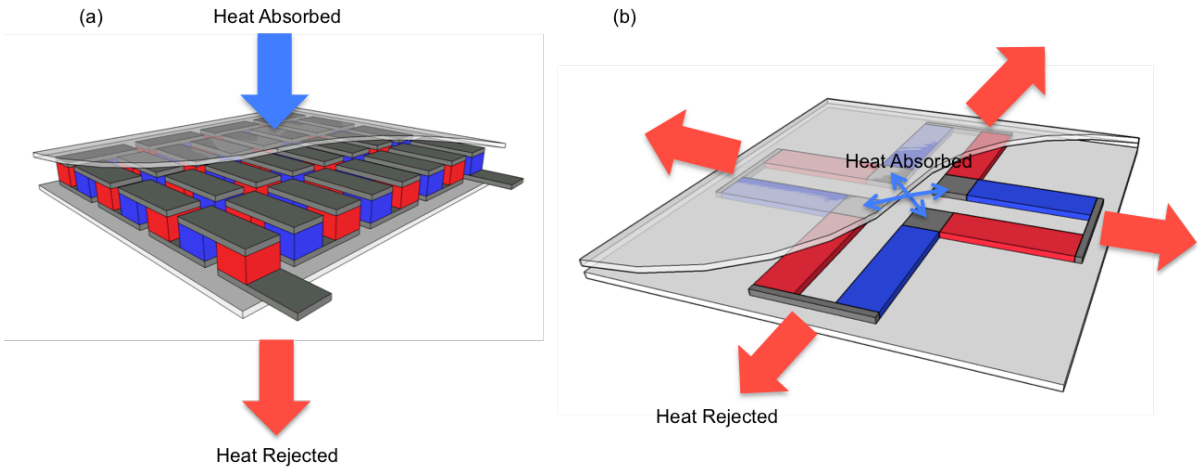

Figure 2.3. (a) Cross-Plane Heat Flow Typical of Bulk TEC and (b) In-Plane Heat Flow in a Thin-Film TEC

Bulk modules are commercially sold in a variety of sizes to meet specified temperature and cooling capacity requirements. A series of conventional, bulk TEC modules manufactured and sold commercially by TE Technology, Inc. are shown in Figure 2.4 [27]. These are typically manufactured on a small-scale level and involve sputtering the TE material onto the substrate and then etching the material into legs. The length of the legs typically ranges from 0.1 to 1 mm thick. The construction of bulk modules can be a time consuming and costly process that is not easily scaled into large-scale manufacturing [28].

This non-automated process involves dicing, soldering, wiring, and intensive placement of material (which are often rare earth minerals) [14], [28]. In addition, a system consisting of a TEC module and heat exchangers or heat sinks on the hot and cold side of the device are required to create continuous cooling via high heat flux across a device [28].

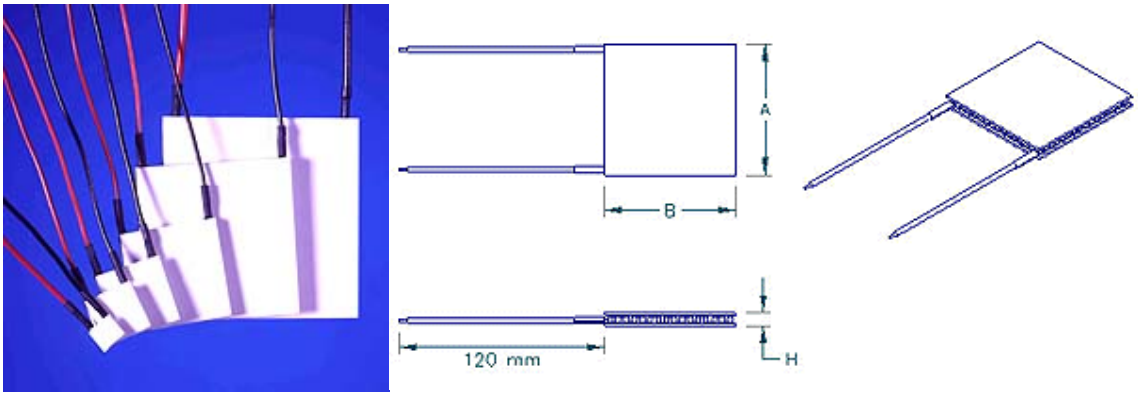

Figure 2.4. Standard TEC Modules [27]

Thin-film devices have been explored as alternatives to the conventional, bulk architecture. Yao et. al describe an in-plane thermoelectric microcooler that is structured like the device in Figure 2.3(b) and built inside a frame that acts as a heat sink [29]. Very high cooling densities, which could be suitable to localized spot cooling or laser cooling applications, can be achieved where the thermocouples meet and heat is absorbed, but heat leakage through the substrates decreases the performance of the device [29].

Thin-film devices are also able to take advantage of the high *ZT* values of superlattice and other nanostructured materials while decreasing the TE material needed to produce a cooling capacity. Returning to Figure 2.2, the most commonly used bulk material (BiTe) has

a *ZT* value of around 1 while superlattices and other complex materials achieve values over 2—a higher *ZT* value translates into greater *COP*s of the overall device. However, as discussed previously, these specialized superlattice and nanostructured material based TE devices are difficult to scale up in manufacturing and often require specialized equipment to produce [15]. Thin-film devices also introduce the possibility of scaling the manufacturing process by printing PEDOT materials on the substrate or using roll-to-roll techniques, but additional architectures need to be explored to maintain a temperature differential and thus improve the efficiency of the device.

To take advantage of thin-film technology while maintaining the ability to control temperatures across a TEC, researchers have introduced novel hybrid architectures made on flexible substrates like polyimide or polyethylene terephthalate (PET). Thin-film devices with cross-plane heat fluxes have been described by Böttner et. al as having "configurations similar to those of bulk thermoelectric modules, albeit with significantly shorter legs and smaller leg cross sections" [26]. This configuration allows for very rapid cooling and less use of material than a bulk device but introduces difficulty in managing the temperatures on the hot and cold sides of the device and overcoming the electrical contact resistances at the ends of the legs. Further exploration of printing materials on substrates, employing roll-to-roll manufacturing techniques, and designing device configurations in a way that better maintains a temperature differential are introduced with these devices.

Researchers at UC Berkeley introduced a prototype of a printed thick-film, composite Bi_2Te_3 TEG with legs printed on a flexible substrate at thicknesses ranging from 100-200 μm thick [21]. The substrate is then rolled, as shown in Figure 2.5(a), to maintain a cross-plane

heat flow across the legs. Lu et. al and Cao et. al introduced similar devices using inkjet printed and screen printed TE material, respectively [19], [20]. Kim et. al also developed a prototype hybrid device that used a spacer, as shown in Figure 2.5(b), to maintain the temperature across the device, and unlike a conventional TEC, electrical charges (current) flow through a polymer PEDOT TE material while heat flow is through the spacer [18]. Lastly, Wei et. al introduced a device where PEDOT material is screen-printed on paper and reportedly powered light-emitting diodes [30]. These examples offer prototypes that are still early in the design process of printable thermoelectrics. The hybrid architecture introduced in this work is similar to these devices, but a specialized manufacturing technique to create a cross-plane heat flux will be used that differentiates the device configuration from these prototypes.

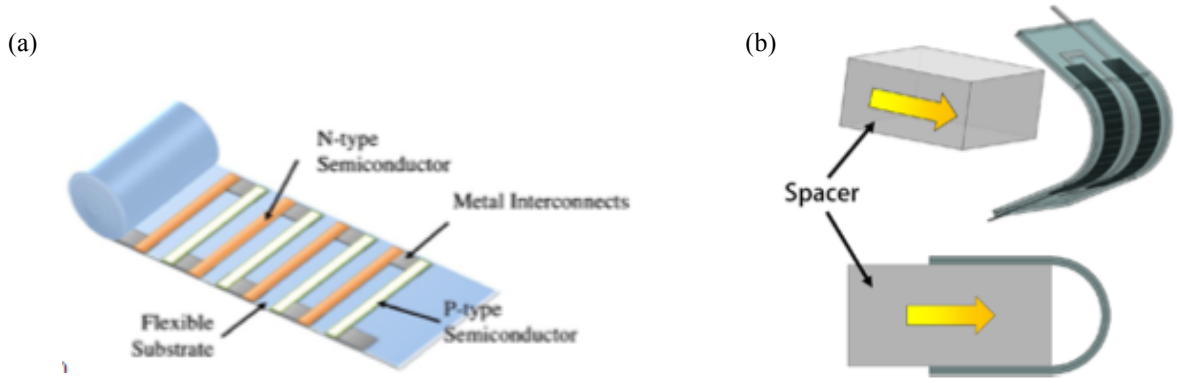

Figure 2.5. Examples of Prototype Device Architectures [18], [21]

Both thin-film and bulk TE devices have their advantages and disadvantages. While allowing for the use of thin-film materials and their high *ZT* values, thin-film devices are

generally limited to localized spot cooling applications. In addition, difficulties in realizing the efficiency of the high *ZT* materials due to heat losses across the substrate limit the performance of the device. In applications that do not require very high cooling densities, cross-plane devices are better suited. Bulk devices are widely available, but are still manufactured on a small level and are not as efficient as alternative methods of cooling or power generation.

Hybrid architectures that are deposited on a substrate in thicknesses like a thin-film and employ roll-to-roll manufacturing techniques but that maintain the cross-plane heat flux of a bulk device offer a promising opportunity for a low-cost, scalable TE device. While each of these have their advantages and disadvantages, researchers continue to work towards achieving better efficiency of both TEGs and TECs through exploration of different device architectures. Hybrid architectures are a promising research area towards producing cost-effective and high performing TECs.

2.3. Roll-to-Roll Manufacturing and Organic Electronics

This section discusses what R2R processing is and how it can be used in manufacturing thermoelectric devices. Additionally, a detailed background about flexible, printable electronics and the suitability of printable materials for hybrid thermoelectric applications is provided. R2R processing is a novel manufacturing technique that draws similarities to the web pressing process used to quickly and efficiently print high volumes of newspapers, books, labels, magazines, and other paper products. This technique and the concept of flexible electronics are still in its infancy, and commercial applications are sparse. Opposed to small-scale, batch production, R2R processing will allow for continuous, large-

scale production of thin-film, printed electronics. Research has focused on the use of this manufacturing technique to produce flexible displays, electronic circuits, transistors, photovoltaic cells, and sensors on flexible substrates. In addition, researchers are exploring the use of R2R processing and organic polymer materials in thermoelectric applications.

In the book *Flexible Electronics: Materials and Applications*, the authors Salleo and Wong describe flexible as having many different qualities: bendable, conformably shaped, elastic, lightweight, non-breakable, roll-to-roll manufacturable, or large-area [22]. The development of flexible electronics began in the 1960s, when silicon wafer solar cells were introduced. Advances continued, and in the 1980s, researchers first begin using R2R processing for solar cell applications. Electronic circuits on flexible substrates appeared in 1994, and in the late 1990s, research into flexible electronics grew rapidly. Finally, organic light-emitting diode (OLED) displays were introduces in the early 2000s [22]. Transistors, Liquid Crystal Displays (LCDs), sensors, actuators, and electronics textiles are additional flexible electronic types noted in [22]. Even more recently, researchers have focused on thermoelectrics on flexible substrates.

These flexible electronics are also printable. Printing technologies use fewer raw materials and can process at a higher volume than traditional photolithography techniques that transfer patterns onto silicon wafers using exposure to UV light. This also allows for large-area, scalable production. Printing methods stem from rotary techniques used in graphic arts and can be applied to R2R processing. Unlike batch printing methods, the rotary techniques allow for scaling to commercial production beyond the laboratory prototypes like those discussed in the previous section. Knife-coating, slot-die coating, rotary screen

printing, ink-jet printing, spray printing, gravure printing, and flexographic printing are available techniques that can be applied to the R2R process.

Each of these techniques have advantages and disadvantages—Søndergaard et. al discuss these in an article on roll-to-roll fabrication of organic materials and provide illustrations of how each technique available to use in R2R processing works, provided in Figure 2.6 [31]. The two coating techniques, knife and slot-die, involve a continuous application of ink on the surface of the substrate whereas the printing techniques allow for patterning of the ink on the substrate. The coating techniques also allow for more precise control of the thickness of the ink as printing is regulated by how quickly the web (the substrate) is moving and how much ink is pumped through the system. Screen printing uses a mesh screen and a squeegee to deposit ink, but rotary screen printing, which allows for faster manufacturing speeds, is better suited to R2R processing. Gravure printing is commonly used for food packaging, wall paper, greeting cards, and magazines and uses surface tension of the ink to transfer ink from cavities to the substrate. Lastly, flexographic printing acts like a stamp by using direct contact of a plate cylinder to the substrate to transfer ink. Doctor blades are used in both flexographic and gravure printing, allowing for better control of ink thickness. Inkjet printing is an additional technique that can be applied in a R2R processing system. In each of these printing techniques, ink viscosity, surface tension, and evaporation rate need to be considered. Screen printing is good for high viscosity inks to prevent the ink from seeping through mesh while gravure and flexography printing requires high viscosity inks.

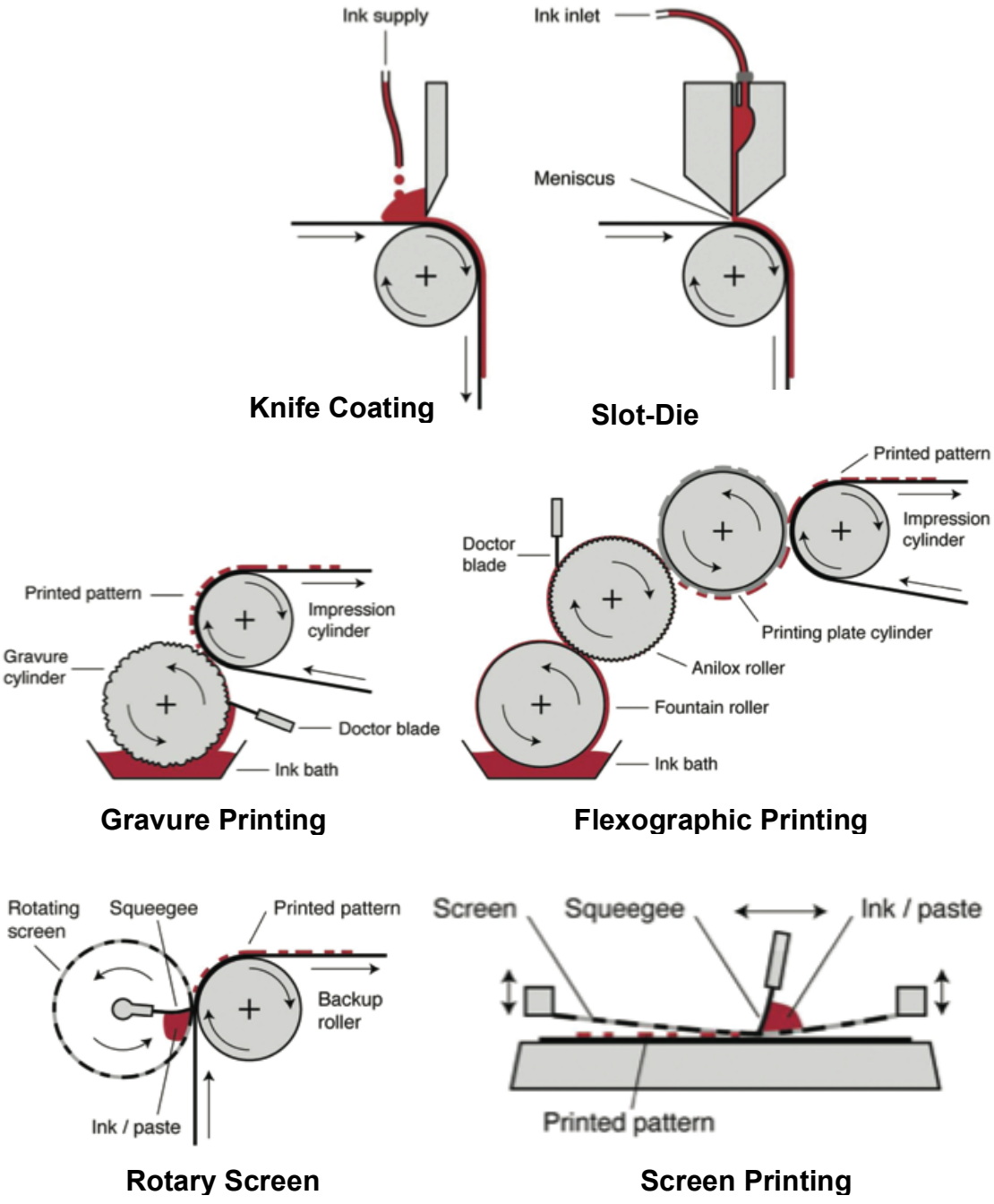

Figure 2.6. Illustrations of Coating and Printing Techniques [31]

As an example of a thermoelectric device developed specifically for R2R processing, Søndegaard et. al present a thermoelectric with flexographic printed silver paste metal interconnects and rotary screen-printed PEDOT [14]. A 60 μm thick PET substrate was used, and the PEDOT material was printed with very small thicknesses around 1.2 μm. The thickness of the material and substrate were described as important aspects of the design as thermal properties and risk of damage to printed layers need to be considered. In this thesis, manufacturing constraints on film thickness are designated by specifications from a rotary screen print manufacturer and are larger than the 1.2 μm layers presented in [14]. Incorporation of spreading resistance will help account for the substrate thermal properties, and considerations for damage will be addressed in future work.

Søndegaard et. al also calculated an energy payback of the device they prototyped. The device needed to generate 0.204 W of to reach an energy payback of one year, but their results on the device were much worse than their goal with an actual energy payback of 3.7 billion years. The authors indicate that organic TEGs will be unlikely to accomplish energy paybacks comparable to the lifetime of the device due to the small temperature tolerances of organic PEDOT, but their conclusions state that R2R processing is a viable method for manufacturing TE devices. In addition, their work focused on TEGs. TECs, which may be more suitable for the low temperature or small temperature differential applications, has not been explored. Through the use of design optimization and continued advancement of TE materials (including printable inorganic materials), further analysis can be done to optimize the performance and cost-effectiveness of TECs and TEGs.

2.4. Design Optimization of TECs

To design a TEC system, designers must consider device configuration, TE materials, manufacturing costs, operating conditions and temperatures, heat exchangers, cooling requirements, and efficiency requirements. Design optimization can play an important role in balancing the trade-offs between conflicting design choices (e.g. cost of a material versus increased *ZT* or maximizing for cooling capacity while sacrificing efficiency) and ultimately reaching a set of design goals. Previous design and optimization research on thermoelectrics has focused on cooling capacity (Q_C) and Coefficient of Performance (*COP*), which measures the efficiency of a heat pump, of bulk TECs and TEGs. More recent attention has been directed towards incorporating costs and other device architectures. Optimization techniques have used analytical methods with derivatives to solve for optimal current, sensitivity analysis, and heuristic methods like genetic algorithms and simulated annealing.

Research focused on the design of TECs identified the importance of the design of heat exchangers in a TEC system. Yamanashi used a standard set of TE equations (based on the heat balance of the flow from the hot side and cold side of the device and the power input), then derived dimensionless quantities for entropy flow, and characterized a TEC system by a dimensionless figure of merit of the TEC and thermal resistances of hot and cold side heat exchangers [32]. The standard set of equations is commonly used throughout the thermoelectric literature as an analytical model and will be presented in Chapter 3 [3]. After analyzing the effects of the thermoelectric properties and heat exchangers and maximizing for *COP* using numerical calculations, Yamanashi found that the hot side heat exchanger has greater effect on performance than the cold side heat exchanger. The research assumed a

constant temperature difference and a constant heat load. Huang, Chin, and Duang used performance curves of actual TEC modules to verify results of optimal current on maximum *COP* and maximum Q_C simulated designs [33]. The performance curves and simulated results indicate that the required heat sink thermal resistance changes with the input current under a fixed cooling capacity. A 43% improvement in *COP* was observed when switching from the least expensive heat sink design to the best available, more expensive heat sink. Both of these articles indicate that a comprehensive analysis of a TEC system, including the TEC device and heat exchangers, is needed when designing a TEC.

Similar to the previously mentioned work, Zhou and Yu maximized *COP* and Q_C separately by allocating thermal conductance of hot and cold heat exchangers [34]. A model including both hot and cold-side heat exchangers is developed and then the optimal current to produce maximum *COP* and, separately, maximum cooling capacity is analytically determined. Huang et. al used the simplified conjugate gradient method to optimize geometric structure of a miniature TEC (3 by 3 mm^2 device cross-sectional area) for maximum Q_C with a constraint on *COP*, and found that leg length should be as small as possible with the area of the TE legs as large as possible [35]. They also provided insight into the effects of current and temperature differentials across the device on performance. Their research indicated that, through the use of optimization, the cooling capacity was improved by two to ten times their original design.

Additional work has used heuristic optimization techniques, including genetic algorithms (GA) and simulated annealing (SA). Genetic algorithms mimic natural selection to evolve a solution to a problem, and simulated annealing imitates a metallurgy process of

heating and controlled cooling of a material to decrease the number of defects. Cheng and Lin used a genetic algorithm to maximize Q_C in a confined volume while treating *COP* and cost (calculated using only TE material costs) as constraints [36]. Leg length, cross-sectional leg area, and the number of thermocouples were the design variables while input current, volume the TEC could consume, and operating temperatures were fixed. Heat exchangers were not included in their analysis, but the authors demonstrated that GAs could be used to improve the cooling capacity of a TEC. Later work by Cheng and Shih extended the use of GAs to an analysis of two-stage TECs [37]. Two-stage TECs are composed of two TEC modules stacked together to achieve very large temperature differences across a device for special applications. Through the consideration of contact and spreading resistances between the two stages, Cheng and Shih reported that maximum Q_C and *COP* could be found by fine-tuning of the design parameters, which only included current through each stage and the ratio of thermocouples between the hotter stage and colder TEC stage.

Nain et. al also performed single objective analysis of TECs using a genetic algorithm [38]. The design variables considered were leg length and cross-sectional area of the TE legs. To distinguish this work from that by Cheng and Lin, this article included a parameter for hot-side heat sink thermal resistance and explored the impact of the heat exchangers on the design of a TEC system. The authors reported that the structural parameters of the TE elements (leg length and area) have significant influence on *COP* and Q_C and that a lower heat sink thermal resistance increases the maximum *COP* and Q_C. Another finding was that longer leg lengths were needed for higher values of heat sink thermal resistance. Reported in the same article, Nain et. al performed a multiobjective analysis of a TEC system using a

Non-dominated Sorting Genetic Algorithm-II (NSGA-II), generated sets of Pareto optimal solutions for different values of hot side heat sink thermal resistance, and demonstrated the trade-off between *COP* and Q_C [38]. In this study, additional model considerations, including spreading resistance and further analysis on heat exchangers, and design variables will be considered that more comprehensively predict and analyze a TEC. Furthermore, cost will be incorporated as a performance objective to assess the value of a TEC beyond just its efficiency (*COP*) and cooling capacity (Q_C).

Research by Khanh et. al tested the effectiveness of genetic algorithms and simulated annealing for single-stage TECs and indicated in a preliminary conclusion that simulated annealing was more robust [39]. Like in previous studies, the design variables considered were leg length, leg cross-sectional area, and the number of thermocouples, and fixed parameters included total volume in which the TEC can be placed, operating temperatures on the hot and cold-sides, current, and material properties. A standard set of thermoelectric equations was used to model the TEC, and heat exchangers were not included in the analysis. However, the bounds on the design variables did allow for consideration of thin-film devices with leg lengths as small as 0.03 mm and leg areas as large as 100 mm^2. When using a GA, many local optimum were found, indicating that the results of the GA may not be reliable. In contrast, SA indicated more consistent solutions over multiple runs of the optimization algorithm, but the researchers indicated their results were unreliable when compared to prior work when using SA for problems with a nonlinear inequality constraint.

Instead of using the aforementioned optimization methods, Venkata Rao and Patel implemented a modified teaching-learning based optimization algorithm to maximize a

weighted sum objective combining *COP* and Q_C for two-stage TECs [40]. This method is based on the effect of teachers on learners in a classroom, where the learners makeup a population, the design variables act as subjects the learners can learn, and the teachers are the best solutions in the population trying to improve the results of the class. Like the two-stage TEC analysis in [37], Venkata Rao and Patel optimized the current through each stage and the ratio of thermocouples between the hotter stage and colder. Research by Abramzon also employed a multistart adaptive random search (MARS) method to optimize TECs for electronic cooling applications [41]. Using the standard model of a TEC with considerations for the thermal resistance between the TEC junctions and the environment, Abramzon considered different scenarios: minimize input power while finding operating temperatures for a given number of thermocouples, maximize Q_C while setting temperatures and defining a power input, minimize input power at a specified temperature and Q_C, and maximize *COP* with the number of thermocouples and the ratio of cross-sectional area to leg length as the design variables. This work demonstrated the use of MARS as applied to TEC design but did not draw definite conclusions into the design of a TEC.

Yazawa and Shakouri, Yee et. al, and LeBlanc et. al have explored the design of TECs and TEGs with a focus on the cost performance of the devices [15], [17], [42]. These studies shift to more practical considerations of TE devices and work towards real world applications. In power generating devices, attention to costs (on a $/W basis) can influence a design just as much as efficiency and power output and present trade-offs designers must consider in the design process. TECs can be analyzed on a $/kWh basis, bringing attention to both capital cost and operating cost. For both TECs and TEGs, opportunities for cost savings

and examination of the effects of costs on design decisions can be explored. The work involving cost analysis of TE systems, however, has primarily focused on energy generating devices with a few insights into coolers developed by Leblanc et. al.

Yazawa and Shakouri explored the maximum power output of a TEG while considering the cost/efficiency trade-offs [17]. The heat exchanger and TEG leg length were co-optimized to count total system performance, and inorganic materials and organic polymers were compared. The goal was to maximize cost per unit of power output ($/W) and mass of the device per unit of power (kg/W) under different heat flux considerations while including the only the cost of both the TE material and the substrate. The authors concluded that the substrate plays a large role in design when the legs take up a small portion of the total cross-sectional area of a device—this ratio of leg area to total device area is called the fill factor—and that polymer materials could prove advantageous in application due to them being low in cost and light in weight.

Yee et. al also introduced a cost per unit of power ($/W) cost metric for TEGs, and optimized the TE leg length and system fill factor for the minimum $/W [42]. This work considered more than just the material cost of the TE material and substrate by incorporating material, manufacturing, substrate, and heat exchanger costs. Manufacturing costs of the materials were gathered using equipment costs and then determining the equipment throughput to arrive at $/kg (volumetric material cost) and $/m^2 (areal material cost) values. The goal was to look beyond the *ZT* values of materials by adding equipment costs incurred during manufacturing. While identifying regions of a performance space where different cost components dominated, the authors concluded that very expensive TE materials can be cost

effective in a TEG system if implemented with short TE legs and small fill factors. While only a first pass analysis of costs, this metric could be used to identify areas of savings by either material selection or heat exchanger choice.

LeBlanc et. al extended the work of Yee et. al to include an analysis of more TE materials and to introduce a cost metric ($/kWh) for TECs [15]. This metric incorporates operating costs into the equation since this is not considered when analyzing TEGs. Additionally, the authors introduced a list of materials, bulk, thin-film, and polymer, and their associated manufacturing costs. However, while concluding that heat exchangers are a major component of the costs of TEGs, heat exchangers were ignored in the analysis of TECs to simplify their analysis. This metric is already seen in thermoelectric literature—Kim and Kim have applied Leblanc et. al's $/W metric to the TEG device architecture seen in Figure 2.5(b) [43]. They found that they could reduce the cost of a device optimized to maximum power by 90% while still producing 65-70% of the maximum power output. Yee et. al's metric and the extensions introduced by Leblanc et. al can be important tools in the design process of a TEC system.

2.5. Summary

In an article on thermoelectric systems, Bell notes the research areas directed towards realizing improvements in the performance of TECs [9]. Improvements in thermoelectric materials, the use of design optimization, and the exploration of alternative device architectures are identified as ways to achieve higher performing TECs. Additionally, roll-to-roll processing has the potential to introduce significant cost saving to the manufacturing of TECs. A background on TE materials available for use in devices is necessary to understand

how a device works and how their costs may affect the cost efficiency and performance outcomes of a TEC system, and an introduction to device architectures seen throughout the literature provides context to the work done in this study. Researchers have introduced cost metrics of TEG and TEC systems that can be used to perform an initial analysis of designs and work towards realizing real world applications.

These cost metrics provide the basis for the cost analysis completed in this study, and the past design optimization research provides a foundation to build on to further explore how a new device architecture can help to realize the potential of TECs. To add to the body of design optimization research on TECs and address the limitations of prior work, this study will incorporate multiple model considerations seen throughout the previously mentioned work and also introduce different performance objectives to begin analysis beyond a purely theoretical standpoint. While LeBlanc et. al introduced the cost metric for TECs, their work did not include heat exchangers in the overall system cost, even though this was noted by other authors as an important design consideration [15]. Works that included heat exchangers and spreading resistance, only considered cost as thermoelectric material cost, ignoring additional manufacturing costs (outlined in LeBlanc et. al's research) in their analysis. These limitations under the context of thermoelectric materials and alternative device architectures provide a motivation for the steps taken in this work. In the next chapter, the standard set of equations for a TEC will be introduced, and the additional model considerations of spreading resistance and heat exchangers will be discussed.

3. MODELING OF THERMOELECTRIC COOLER

In this chapter, the device architecture analyzed in this study, the set of analytical equations used to model a TEC, and the metric for analyzing the total system cost will be introduced. A standard set of equations is widely used to model thermoelectric coolers [3]. In addition to cost two important performance parameters are the cooling capacity (Q_C) and the coefficient of performance (*COP*), which is a common performance indicator of any refrigerator.

3.1. Device Architectures

As discussed previously, a TEC module is composed of multiple thermocouples. The p-type and n-type legs are connected electrically in series, via metal interconnects, and thermally in parallel. The legs and the metal contacts are then sandwiched between an insulating substrate, typically alumina ceramic. The hybrid architecture studied here is similar in structure to a bulk device (see Figure 2.4 for example of bulk device) with differences in the geometric factors, manufacturing techniques, and material choices.

The structure is similar in that cross-plane heat flux is maintained across p-type and n-type legs connected electrically in series and thermally in parallel. However, the length, width, and thickness of the legs are changed from a pellet shape sandwiched between a ceramic substrate to a thin material printed on a PET substrate. Material choices of the hybrid device are also limited to materials that are printable. It is hypothesized that these changes in structure and device properties from a bulk device to a hybrid device will make the hybrid device suitable for applications requiring a very low heat flux over large areas since each leg

of the hybrid device occupies a larger footprint than a bulk TEC leg, resulting in less thermocouples for a given area.

The architecture for the hybrid TEC maintains the cross-plane heat flux while taking advantage of R2R processing. As discussed in the background, bulk devices are not produced via an automated process. With the hybrid device, using R2R processing, TE materials can be printed on the substrate in a scalable manner. By maintaining the cross-plane heat flux, the hybrid device with leg lengths ranging from 10 to 20 mm will be able to maintain more significant temperature differences across the TE legs than other thin-film devices with leg-lengths under a few hundred microns. The TE materials will be rotary screen printed on a flexible plastic (PET) substrate in thicknesses between 50 and 250 μm with a leg width over 10 mm and a leg length between 10 and 20 mm [44]. Based on data from a manufacturer at a 250 mm print width with an ink pump and ink level control, the unit equipment cost of a rotary screen printer is approximately $73,000 [45]. Figure 3.1(a) depicts the printing pattern of the material on the PET substrate. The process presented here is hypothetical, but the approach is supported by prior work in [14], [21], [22], and [31].

A silver paste ink can be used to create the metal interconnects [14]. After printing on one layer of PET substrate, the TE layer is laminated with two more PET layers to sandwich the legs. The module is then processed to shape the device in a way that maintains the cross-plane heat flux like a bulk device. The final device configuration for a hybrid TEC and a bulk TEC are given in Figure 3.1 (a) and (b), respectively.

(a)

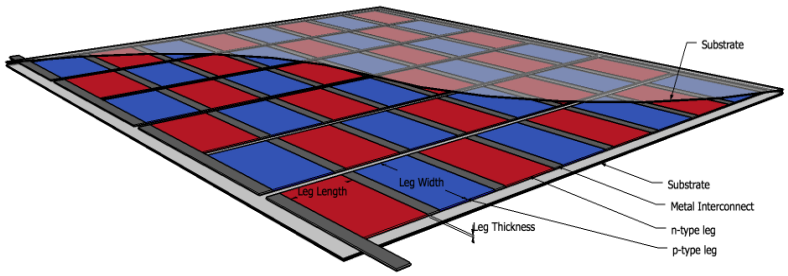

(b)

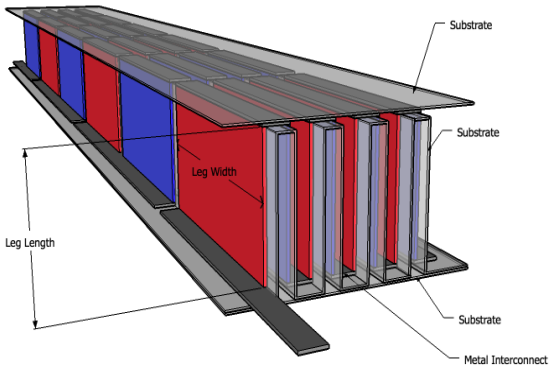

(c)

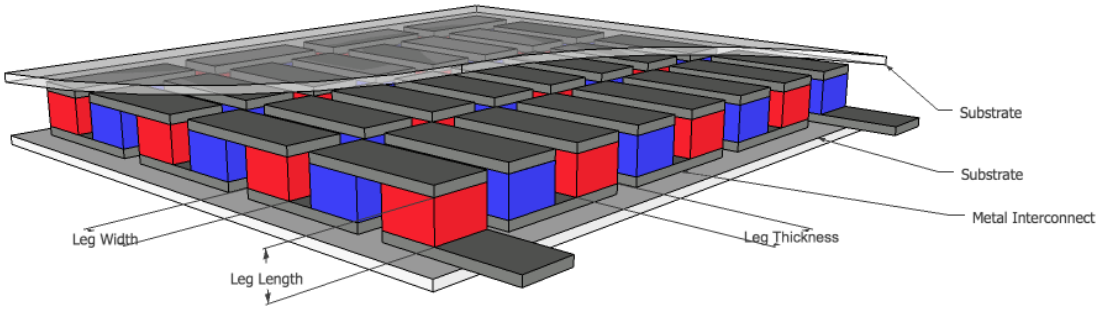

Figure 3.1. Illustrations of (a) Printing Pattern of Material on Substrate, (b) Hybrid TEC after Processing into Final Form, and (c) Bulk TEC

3.2. Fundamental Modeling

The basic structure of a bulk TEC and the hybrid architecture being analyzed are the same. Therefore, the fundamental model used throughout thermoelectric literature will be used for both architectures, with additional considerations for spreading resistance and modeling of the heat exchangers [3]. As current is passed through the thermocouples, heat is absorbed at the cold side of the device (defined by temperature T_C) and rejected at the hot side of the device (defined by junction temperature T_H and ambient temperature T_∞). This phenomenon is driven by the Peltier effect. Figure 3.2 provides a basic diagram of a TEC system aligned with the equivalent thermal resistance circuit model.

Heat balance between Q_C and Q_H provide the foundation for the standard analytical model of a TEC with power input P. Thermal resistance of the heat exchanger (R_{HX}) and thermoelectric elements (R_{TE}) as well as the spreading resistance from the substrate (R_{spread}) contribute to the total thermal resistance in the model. Another phenomenon present in TE devices is the Thomson effect, which describes the rate of generation of reversible heat across a device. The Thomson effect is neglected in this study as it has been shown that, for a wide range of temperatures, models incorporating the Thomson effect show close agreement with the standard set of TE equations not considering the effect [46]. For commercially available TECs, the Thomson effect provides little improvement or degradation in Q_C and *COP* results.

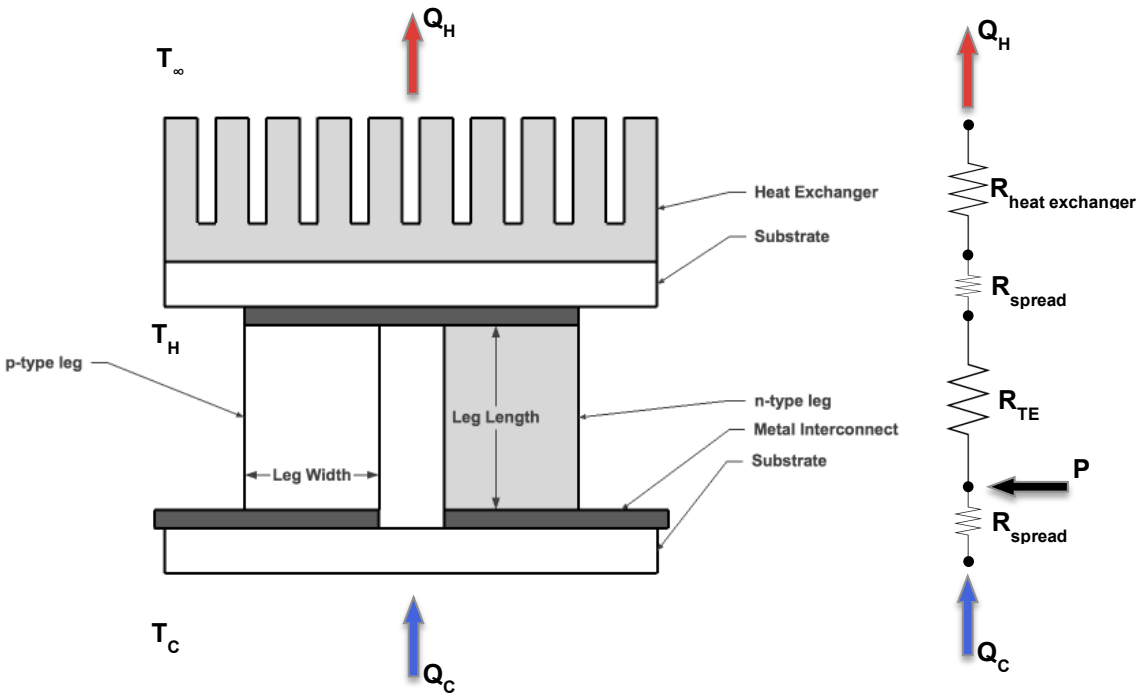

Figure 3.2. Basic Diagram of a TEC and the Equivalent Thermal Resistance Circuit of the System

Cooling using a TEC must overcome Joule heating (where the flow of electric current through the TE elements releases heat) and the heat conduction through the TEC legs (known as the Fourier effect). Half of the Joule heating flows to each of the junctions of the TEC. Combining the Peltier effect, Joule heating, and the Fourier effect, the heat absorption into the device, Q_C, is given in Eq. (3.1). In the equations below, Joule heating is designated by the term $\frac{1}{2}I^2R$, where R is the total thermal resistance as described by Figure 3.2(a) The Fourier effect is described by $K(T_H - T_C)$, and the Peltier effect by $I\alpha T_C$. The Peltier effect term includes the Seebeck coefficient (α), and the Fourier effect includes a term accounting for the thermal conductivity of the device (K). Lastly, the Joule heating term accounts for the electrical resistivity (R). Similar to the heat absorption on the cold side of the device, the

energy balance equations give the heat rejected at the hot side, given in Eq. (3.2). The heat conduction through the legs is between temperatures T_H and T_C. In these equations, *N* is the number of thermocouples, and *I* is the input current.

$$Q_C = N\left[I\alpha T_C - K(T_H - T_C) - \frac{1}{2}I^2R\right] \tag{3.1}$$

$$Q_H = N\left[I\alpha T_H - K(T_H - T_C) + \frac{1}{2}I^2R\right] \tag{3.2}$$

To simplify the analytical model, a heat sink is only considered on the hot side of the TEC. This is a common assumption made in the analysis of a TEC and was a tactic used in the design optimization research discussed in the background [39]. An infinite sink is assumed on the cold side, and the known ambient air temperature (T_∞) along with the heat exchanger heat transfer coefficient (U) and cross-sectional area of the device are used to determine the hot-side junction temperature (T_H), calculated by Eq. (3.3).

$$T_H = Q_H \frac{1}{UA} + T_\infty \tag{3.3}$$

The electrical power applied to the device needs to overcome the Seebeck voltage that results from the temperature difference between the junctions and the electrical resistance of the TE elements. The power input, P is shown in Eq. (3.4). An energy balance of the system gives $P = Q_H - Q_C$.

$$P = N[I\alpha(T_H - T_C) + I^2R] \tag{3.4}$$

The coefficient of performance, given in Eq. (3.5), expresses the efficiency of a TEC and is given by the heat absorbed by the device divided by the power expenditure into the device. This is a prevalent expression used to describe the efficiency of any heat pump.

$$COP = \frac{Q_C}{P} \tag{3.5}$$

This set of equations describes the technical performance of a TEC. In addition to these equations, it is necessary to calculate the total Seebeck coefficient, thermal conductivity, and electrical resistivity of the device. The next two sections describe these properties as well as the additional consideration of spreading resistance.

3.2.1. Spreading Resistance

TE legs only occupy a fraction of the footprint of the substrate of the TEC—the fill factors (a ratio bounded between 0 and 1 that is the cross-sectional area of the TE legs divided by the cross-sectional area of the device) considered in this study range from small values nearing 0.01 to large values approaching 0.8. The small fill factors reduce the heat flow across the device; thus, to work towards a more accurate model, the thermal spreading resistance needs to be accounted for [17]. Widely used in electronics applications, a model developed by Song et. al is applied to this TEC application as it allows for calculations for varying geometries and has proven to be an accurate and simple approximation for spreading resistances [16].

To calculate spreading resistance, which is not a linear relationship to fill factor, Song et. al first outline steps for converting the rectangular areas of the TE legs (A_{TE}) and the device (A) to a circular geometry. The authors cite previous work that indicates the circular geometry is applicable to other equivalent geometries. This conversion is given by Eq. (3.6) and (3.7) and depicted in Figure 3.3.

$$a = \sqrt{\frac{A_{TE}/2}{\pi}} \tag{3.6}$$

$$b = \sqrt{\frac{A/2}{\pi}} \tag{3.7}$$

Given by Eq. (3.8) and (3.9), dimensionless solutions for contact radius (ε) and plate thickness (τ) are then determined. These dimensionless parameters are presented by Song et al. to simplify the presentation of solutions [16].

$$\varepsilon = \frac{a}{b} \tag{3.8}$$

$$\tau = \frac{d_s}{b} \tag{3.9}$$

An empirical parameter (λ_c) is calculated followed by a dimensionless parameter (Φ_c) and dimensionless constriction resistance (ψ). These three equations represent a simple approximation, noted to be in agreement with numerical solutions, to analytical solutions developed by [16] and are given by Eq. (3.10)-(3.12). Finally, the spreading resistance (R_{spread}) is determined by Eq. (3.13).

$$\lambda_c = \pi + \frac{1}{\sqrt{\pi}\varepsilon} \tag{3.10}$$

$$\Phi_c = \frac{\tanh(\lambda_c \tau) + \frac{\lambda_c}{Bi}}{1 + \frac{\lambda_c}{Bi}\tanh(\lambda_c \tau)} \tag{3.11}$$

$$\psi = \frac{\varepsilon\tau}{\sqrt{\pi}} + 0.5(1-\varepsilon)^{3/2}\Phi_c \tag{3.12}$$

$$R_{spread} = \frac{\psi}{\sqrt{\pi}} \kappa_s a \tag{3.13}$$

In these equations, κ_s is the substrate thermal conductivity, d_s is the substrate thickness, and *Bi* is the Biot Number, which is set to 0.1 under the assumption that the temperature gradient inside the substrate is negligible.

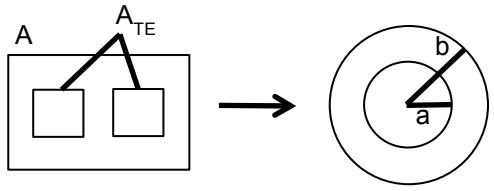

Figure 3.3. Illustration of Variables Used to Calculate Spreading Resistance

3.2.2. Material Properties

Additionally, the fundamental equations for TEC analysis are a function of material properties. The thermal resistance through the TE legs, R_{TE}, is given in Eq. (3.14). The electrical resistance (R), total thermal conductivity (K) as a function of the spreading resistance (R_{spread}) and thermal resistance through the TE legs (R_{TE}), and Seebeck coefficient (α) are given in Eq. (3.15), (3.16), and (3.17).

$$R_{TE} = \frac{1}{(\kappa_p + \kappa_n)\frac{tw}{L}} \tag{3.14}$$

$$R = (\rho_p + \rho_n)\frac{L}{tw} \tag{3.15}$$

$$K = \frac{1}{R_{TE} + R_{spread}} \tag{3.16}$$

$$\alpha = \alpha_p - \alpha_n \tag{3.17}$$

In these equations, t, w, and L are leg thickness, width (tw is the cross sectional area of the TE leg), and length, respectively. Properties of the p-type and n-type legs (designated by the subscripts p and n) comprise the total material properties: κ represents the material thermal conductivity, ρ the electrical conductivity, α the Seebeck coefficient.

Several common assumptions are made in the development of this analytical model [3]. The p-type and n-type TE elements have the same basic geometries, rectangular shapes sharing the same leg length, thickness, and width. The Seebeck coefficient, thermal conductivity, and electrical resistivity of the TE material are considered temperature independent [4]. For simplicity, the thermal and electrical contact resistances of the substrate and the metal are treated as negligible, and as stated previously, the Thomson effect is also neglected [3]. The same set of equations is used to evaluate the performance metrics for both the hybrid and bulk architectures. The overarching structure of the devices remains the same, but the geometries (e.g. leg thickness, width, and length) and material properties are altered to reflect the different architectures. While this is a simplification, it allows for a first pass comparison of the advantages and disadvantages of both the hybrid and bulk architectures.

3.3. Cost Metric

The cost breakdown for a TEC, and the parameters that contribute to the cost, are given in Figure 3.4. The cost metric analysis is derived from the work by Yee et. al and LeBlanc et. al [15], [42]. While their work considered heat exchangers in the cost metric for TEGs, a contribution of this work is to also incorporate heat exchangers into the analysis of a TEC by using a similar procedure as that for TEGs. This work presents a novel contribution to incorporate heat exchangers and their associated cost into the analysis of a TEC system.

The total cost of a TEC can be subdivided into operating cost and capital cost. The operating cost considers the efficiency of a device through its *COP* as well as the cost of the power source. Capital cost can be broken into three segments: TE material, substrate, and heat exchanger. This cost metric is measured by $/kWh of cooling.

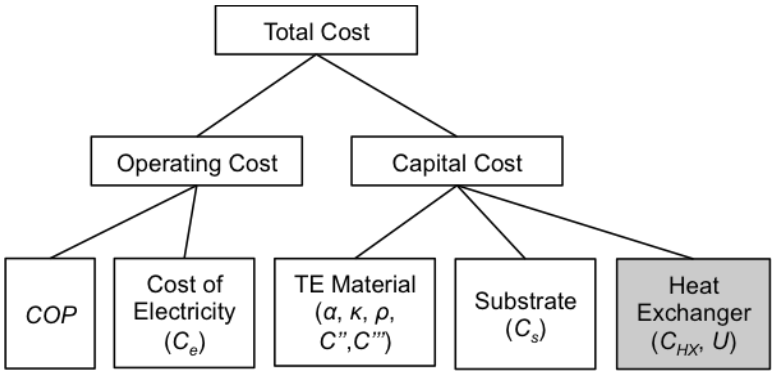

Figure 3.4. Breakdown of the Total Cost of a TEC System

Device geometry and material, manufacturing, and heat exchanger costs are considered key components in a cost metric for a TE. Yee et. al, present a cost metric that includes these components while incorporating volumetric material costs (C'''), areal material costs (C''), and heat exchanger/ceramic substrate costs (C_{HX}) [42]. Volumetric and areal costs were determined by considering equipment prices (for ball milling, melt spinning, spark plasma sintering, dicing, metallization, microfabrication, and screen printing) and derived heat exchanger costs from actual engineering data on heat exchangers compiled in [47]. To analyze the total system cost of a TEC and to study the bulk and hybrid architectures, which have different substrate materials, the heat exchanger/substrate component of Yee et. al's

cost metric is separated into heat exchanger cost and substrate cost (C_s). This allows for a deeper analysis of the effects of the heat exchanger on system cost and for the use of different substrate materials (ceramic for the bulk device and PET for the hybrid device). Using the volumetric (C'''), areal (C''), heat exchanger (C_{HX}), and substrate cost (C_s) components, the overall system cost (C) of a TEC is given in Eq. (3.18). An operating cost, in terms of \$/hr, based on the cost of electricity (C_e) and power input into a device (P) can also be derived and is given in Eq. (3.19)

$$C_{capital} = N[(C'''L + C'')wt + C_{HX}UA + C_sA] \tag{3.18}$$

$$C_{operating} = C_eP \tag{3.19}$$

LeBlanc et. al extended this basic capital cost by providing a list of common TE materials [15]. The materials used in this analysis and the associated manufacturing costs compiled by LeBlanc et. al are given in Chapter 4. These manufacturing costs are an appropriate lower bound for the estimated costs of manufacturing the thermoelectric material [15], [48]. The volumetric material costs (C''') include the cost of the thermoelectric material on a \$/kg basis and volumetric manufacturing costs like ball milling and hot pressing. Likewise, the areal material costs (C'') include the cost of metallization and areal manufacturing costs such as dicing and cutting.

These costs are associated with the price of the equipment used in manufacturing and the quantity of TE devices processed on that equipment. LeBlanc et. al provided the cost of equipment, which is given in Table 3.1, and material cost was gathered from raw material costs reported in the *U.S. Geological Survey* [15]. In addition, Leblanc et. al derived heat exchanger costs from data in Shah and Sekulic's work on heat exchanger design [47], [49].

The heat exchanger cost is in $/(W/K) and is closely related to the heat transfer coefficient of the exchanger as more complex designs increase the cost of the exchanger.

Table 3.1. Manufacturing Process and Associated Equipment Cost (adapted from [15])

	Process	Equipment Cost ($)
Volumetric Processing	Ball Milling	40,000
	Melt Spinning	135,000
	Spark Plasma Sintering	400,000
Areal Processing	Dicing	150,000
	Metallization	200,000
	Molecular Beam Epitaxy	600,000
	Screen Printing	50,000

COP is considered in order to calculate an operating cost. Continuous operation over a 20-year period (the industry standard for the mean time between failures is over 200,000 hours) is used, so the amortized cost can be simplified. This cost metric, developed by LeBlanc et. al and given in Eq. (3.20), is expressed in $/kWh and includes the capital cost amortized over the lifetime and the lifetime operating cost for a given cooling capacity. In this equation, *r* is the amortization rate.

$$H = \frac{C_{operating}}{Q_C} + r\frac{C_{capital}}{COP \cdot P} \tag{3.20}$$

3.4. Summary

After breaking down Yee et. al's overall system cost into TE elements, heat exchanger, and substrate costs, both traditional methods of manufacturing bulk devices and screen printing of hybrid structures can be analyzed. Additionally, LeBlanc et. al did not include heat exchangers in their analysis of TECs but found that the heat exchanger is a large

component of the cost of TEGs—to simplify their model, they treated heat exchangers on the hot and cold side of the device as infinite sinks. The heat exchanger can also greatly impact the performance characteristics of a TEC, so in this work, a heat exchanger on the hot side of the device is considered. Consequently, the cost metric and TEC model used in the literature was modified to include heat exchangers, allow for different device geometries, and incorporate additional substrate materials. The fundamental set of equations, material property calculations, and an established cost metric provide the foundation for the analysis in this study.

4. METHODOLOGY AND PROBLEM FORMULATION

This chapter describes the formulation of optimization problems used to explore the performance and design spaces of bulk and hybrid TECs. Several different problems are considered to glean information on the design of a TEC and to work towards real world applications. First a multiobjective problem is formulated with the goals of minimizing cost and maximizing cooling capacity. To further explore the performance space, a single objective optimization problem is formulated with the goal of minimizing the device area for a given cooling capacity. To perform a more thorough analysis of TEC cost, two single objective problems are formulated that minimize capital cost and operating cost. The results from the different optimizations and example design scenarios lead to a better understanding of the geometric factors, TE materials, heat exchanger components, and operating current of an entire TEC system for the hybrid and bulk architectures.

In addition, the introduction of genetic algorithms (GA) and simulated annealing (SA) to analyze cost brings a more thorough examination of the single objective optimization problems. Khanh et. al compared these two heuristic techniques in a TEC problem using a similar mathematical model and indicated that the GA often settled on local optimum instead of converging to the global optimum [39]. However, issues finding a solution close to an optimum under constrained problems using SA were also observed as the solutions did not approach values for cooling capacity (Q_C) found using a GA. To ensure that the problem converges to an optimal solution and solutions can be used to gain insights into the design of a TEC, both approaches will be represented in this work.

4.1. General Problem Formulation

The purpose of design optimization is to lead engineers to the best possible solution for a given problem formulation. Each problem has common aspects: one or more objectives, constraints, and design variables. An algorithm is used to find the combination of design variables that produces the optimal measurable performance under a set of constraints. The objectives have measurable performance, and in this study, a few different objectives from the fundamental model equations and the cost metric are considered. In some problems, many local optimum exist, but global optimization algorithms like genetic algorithms (GAs) and simulated annealing (SA) are applied to search for the global maximum or minimum. In addition, an optimization problem can be constrained or unconstrained, and design variables can be continuous or discrete. The general form of the problem statements for this study is given by Eq. (4.1).

$$\begin{aligned} &\text{Minimize:} && f_i(\boldsymbol{x}),\ i = 1,\ldots,k \\ &\text{Subject to:} && g_i(\boldsymbol{x}) \le 0,\ i = 1,\ldots,m \\ & && h_i(\boldsymbol{x}) = 0,\ i = 1,\ldots,p \\ & && x_i^{min} \le x_i \le x_i^{max},\ \mathrm{i} = 1,\ldots,\mathrm{n} \end{aligned} \tag{4.1}$$

The objective functions are given by $f(\boldsymbol{x})$. Inequality constraints are designated by $g_i(\boldsymbol{x})$ and equality constraints are defined by $h_i(\boldsymbol{x})$. $\boldsymbol{x}$ is a vector of design variables where lower bounds and upper bounds are set as side constraints to define the feasible values of the design variable.

Different objectives pertaining to cooling performance, cost, and cross-sectional area of a device will be analyzed to explore the performance space of a TEC. The design variables considered are the:

- thickness of the TE leg (t),
- width of the TE leg (w),
- length of the TE leg (L),
- space between the legs (δ),
- input current (I),
- p-type material ($material_{p\text{-}type}$),
- n-type material ($material_{n\text{-}type}$),
- number of thermocouples (N),
- and, the overall heat transfer coefficient of the heat exchanger (U).

Bounds for the optimization algorithm of a bulk TEC are set by manufacturing constraints and those established in the literature. In some situations, current would not be a design variable as it is dictated by the device used to power the TEC. For example, if a 13 V car battery is used to power the system, the current needs to be selected that provides the necessary wattage based on the equation $P=IV$. However, current is used in this work as the formulas for cooling performance and device efficiency are functions of current. Twenty-five different material choices, and their associated cost, Seebeck coefficient, thermal conductivity, and electrical resistivity, were investigated for the bulk optimization problem. These are listed in Table 4.1. The side constraints used in the optimization problem will be given with each formal problem statement.

Table 4.1. Thermoelectric Material Properties and Cost

Bulk Material Selection								
Material	**Type**	**α (V/K)**	**ρ (Ω mm)**	**κ (W/mm-K)**	**C''' ($/mm^3)**	**C'' ($/mm^2)**	**No.**	**Ref.**
Bi_2Te_3	Bulk	-0.000227	0.011474864	0.00157	0.000889565	0.00016823	1	[21]
$Bi_{0.52}Sb_{1.48}Te_3$	Bulk	0.000202	0.007702973	0.00141	0.000865743	0.00016823	2	[21]
$AgPb_{18}SbTe_{20}$	Bulk	-0.000121	0.005076142	0.00228	0.00077717	0.00016823	3	[21]
SiGe	Bulk	0.000117	0.01075963	0.00495	0.003044917	0.00016823	4	[21]
$Mg_2Si_{0.6}Sn_{0.4}$	Bulk	-0.000089	0.00513901	0.0033	1.68306E-05	0.00016823	5	[21]
$MnSi_{1.75}$	Bulk	0.000183	0.127129418	0.00234	7.33212E-06	0.00016823	6	[21]
$Ba_8Ga_{16}Ge_{28}Zn_2$	Bulk	-0.00011	0.033696128	0.00139	0.003123358	0.00016823	7	[21]
$Ba_8Ga_{16}Ge_{30}$	Bulk	-0.000035	0.006281802	0.00172	0.003230061	0.00016823	8	[21]
$Ba_7Sr_1Al_{16}Si_{30}$	Bulk	-0.000023	0.00569833	0.00237	0.000005346	0.00016823	9	[21]
$CeFe_4Sb_{12}$	Bulk	0.000074	0.004444642	0.0026	0.000262299	0.00016823	10	[21]
$Yb_{0.2}In_{0.2}Co_4Sb_{12}$	Bulk	-0.00013	0.006144016	0.00325	0.000193688	0.00016823	11	[21]
$Ca_{0.18}Co_{3.97}Ni_{0.03}Sb_{12.40}$	Bulk	-0.000124	0.005062778	0.00571	9.3016E-05	0.00016823	12	[21]
$(Zn_{0.98}Al_{0.02})O$	Bulk	-0.000084	0.01173282	0.04073	0.000020128	0.00016823	13	[21]
$Ca_{2.4}Bi_{0.3}Na_{0.3}Co_4O_9$	Bulk	0.000124	0.093826234	0.00201	0.00017294	0.00016823	14	[21]
$Na_{0.7}CoO_{2-\delta}$	Bulk	0.000081	0.003024529	0.01993	0.000195925	0.00016823	15	[21]
$Zr_{0.25}Hf_{0.25}Ti_{0.5}NiSn_{0.994}Sb_{0.006}$	Bulk	-0.000208	0.012187988	0.00286	8.06371E-05	0.00016823	16	[21]
$Zr_{0.5}Hf_{0.5}Ni_{0.8}Pd_{0.2}Sn_{0.99}Sb_{0.01}$	Bulk	-0.000103	0.004784689	0.00464	9.1203E-05	0.00016823	17	[21]
$Ti_{0.8}Hf_{0.2}NiSn$	Bulk	-0.000115	0.042971939	0.00405	8.64239E-05	0.00016823	18	[21]
$Bi_{0.52}Sb_{1.48}Te_3$	Nanobulk	0.000224	0.013176967	0.00068	0.00087975	0.00016823	19	[21]
$(Na_{0.0283}Pb_{0.945}Te_{0.9733})(Ag_{1.11}Te_{0.555})$	Nanobulk	0.000069	0.01140576	0.00171	0.000748177	0.00016823	20	[21]
$Si_{80}Ge_{20}$	Nanobulk	0.000114	0.011866619	0.00246	0.001303838	0.00016823	21	[21]
$Mg_2Si_{0.85}Bi_{0.15}$	Nanobulk	0.000098	0.008305648	0.00752	3.34809E-05	0.00016823	22	[21]
Si	Nanobulk	-0.000064	0.004816492	0.0128	9.7627E-06	0.00016823	23	[21]
$Mn_{15}Si_{28}$	Nanobulk	0.000111	0.029804483	0.00275	1.09881E-05	0.00016823	24	[21]
PEDOT:PSS	Polymer	0.00021	0.135135135	0.00037	0.00000051	0.00000476	25	[9]
Hybrid Material Selection								
Material	**Type**	**α (V/K)**	**ρ (Ω mm)**	**κ (W/m-K)**	**C''' ($/mm^3)**	**C'' ($/mm^2)**		**Notes**
PEDOT:PSS	Polymer	0.00021	0.135135135	0.37	0.00000051	0.00000476	26	[9]
Bi_2Te_3	Composite	0.0001585	0.1621645	0.24	0.000865743;	0.00000476	27	[27]

The structure of the formulated problem for the hybrid architecture is identical to that of the bulk architecture, but the side constraints are changed to reflect the changes in geometry of the TEC and the different TE materials choices suitable for a bulk or hybrid device. As discussed previously, length, width, and thickness of the legs of a bulk device are a pellet shape sandwiched between a ceramic substrate. The hybrid device is composed of a

thin layer of TE material printed on a PET substrate. Additional manufacturing considerations for screen-printed inks and processing of the PET substrate are also considered when setting the bounds on the design variables.

Two different material choices, and their associated cost, Seebeck coefficient, thermal conductivity, and electrical resistivity, were available for the hybrid optimization problem. The printable TE material limits the material options for the hybrid device. A BiTe-polymer composite printable material introduced by Chen et. al is introduced to the optimization for printable, hybrid TECs, and PEDOT material properties are updated to reflect the results from Bubnova et. al [13][21]. To use BiTe as a printable solution, which has only recently been the focus of extended research, BiTe is mixed with polymer binders and solvents—the result is a composite TE material with a *ZT* value of 0.18 [21]. These are also listed in Table 4.1.

Operating temperatures are set to an ambient temperature of 20°C with the cold side temperature at 0°C. Alumina ceramic is the substrate for the bulk device as it standard on commercially available devices and those discussed throughout the TEC literature [3]. PET plastic is the substrate for the hybrid architecture since this is a suitable material for R2R manufacturing and is common through flexible electronic applications [22]. Table 4.2 details the properties and design parameters found in both the fundamental TE equations and the cost model.

Table 4.2. Device Properties and Operating Parameters Used in Analysis

Property	Value	Ref.
T_∞	20°C	-
T_C	0°C	-
C''_{bulk}	\$168.23/m^2	[15]
C''_{hybrid}	\$4.76/m^2	[15]
C_{HX}	\$7.60/(W/K)	[15]
C_e	\$0.1035/kWh	[50]
$C_{s,bulk}$	\$0.8625/m^2	[49]
$C_{s,hybrid}$	\$0.3985/m^2	[51]
C_{HX}	\$7.60/(W/K)	[15]
$d_{s,bulk}$	0.5 mm	[8]
$d_{s,hybrid}$	125 μm	-
$k_{s,bulk}$	30 W m^{-1} K^{-1}	[52]
$k_{s,hybrid}$	0.15 W m^{-1} K^{-1}	[53]
r	3% annually	[15]

4.2. Multiobjective Optimization

With multiple objectives, the solution to an optimization problem is no longer a single point, as trade-offs between the different objectives may exist. A nondominated design point is known as a Pareto optimal solution, meaning the solution cannot be improved with respect to one objective without worsening at least one other objective. The Pareto set is all nondominated design points. A feasible design variable vector, x, is a Pareto optimal solution if and only if there is no feasible design variable vector, x$'$**,** with the characteristics,

$$f_i(x') \leq f_i(x) \text{ for all i, i = 1,…,n} \quad (4.2)$$

$$f_i(x') < f_i(x) \text{ for at least one i, i = 1,…,n}$$

where n is the number of objectives. The Pareto frontier thus represents the set of Pareto optimal solutions, or the feasible designs where no other solutions exist in which

simultaneous improvement in all objectives can occur. In this study, a genetic algorithm based on NSGA-II is used to find the optimum set of nondominated design points [54].

The first step towards gaining a better understanding of how each architecture performs is to use the multiobjective optimization results to explore the design and performance spaces. It is expected that the hybrid architecture will be better suited to low cooling density but large area applications, since it is inexpensive to scale up in size but is limited to low *ZT* thermoelectric materials like BiTe-polymer composite solutions and PEDOT polymer. The goal of the optimization problem is to determine the optimal device parameters to maximize cooling capacity, Q_C from Eq. (3.1), and minimize the total device cost, H from Eq. (3.20). In considering these two objectives simultaneously, optimization of a single-stage TEC will be presented that accounts for the trade-offs between the comprehensive costs and performance of the system.

Since the same fundamental model is used to examine the bulk and hybrid devices, the architectures are differentiated by changing the bounds on the design variables. These variables allow for the consideration of different TE materials and alternations to device parameters (e.g. PET substrate instead of alumina ceramic substrate). Bounds for the optimization algorithm of a bulk TEC are set by manufacturing constraints and those established in the literature [3], [8], [36], [39]. Twenty-five different material choices (which are designated by numerical values corresponding to the numbers listed in Table 4.1) and their associated cost, Seebeck coefficient, thermal conductivity, and electrical resistivity, were investigated for the bulk optimization problem. Additional manufacturing

considerations for screen-printed inks and processing of the PET substrate are included when setting the bounds on the design variables for the hybrid problem [14], [15], [21], [22].

Two different material choices (given in Table 4.1), and their associated cost, Seebeck coefficient, thermal conductivity, and electrical resistivity, were available for the hybrid optimization problem. The problem statement for this optimization problem is given by Eq. (4.3) for the bulk device and Eq. (4.4) for the hybrid architecture.

$$\begin{aligned} \text{Minimize:} \quad & f_1 = -Q_C \\ & f_2 = H \\ \text{Subject to:} \quad & 0.5 \text{ mm} \le t \le 0.8 \text{ mm} \\ & 0.5 \text{ mm} \le w \le 0.8 \text{ mm} \\ & 0.1 \text{ mm} \le L \le 1 \text{ mm} \\ & 0.1\text{mm} \le \delta \le 2 \text{ mm} \\ & 0.1 \text{ A} \le I \le 10 \text{ A} \\ & 1 \le material_{n\text{-}type} \le 25 \text{ where } material_{n\text{-}type} \in \mathbb{Z} \\ & 1 \le material_{p\text{-}type} \le 25 \text{ where } material_{p\text{-}type} \in \mathbb{Z} \\ & 1 \le N \le 10000 \\ & 0 \le U \le 100 \end{aligned} \tag{4.3}$$

Minimize: $f_1 = -Q_C$ (4.4)

$f_2 = H$

Subject to: $50\ \mu m \leq t \leq 250\ \mu m$

$10\ mm \leq w \leq 20\ mm$

$10\ mm \leq L \leq 20\ mm$

$0.1 mm \leq \delta \leq 2\ mm$

$0.1\ A \leq I \leq 10\ A$

$26 \leq material_{n\text{-}type} \leq 27$ where $material_{n\text{-}type} \in \mathbb{Z}$

$26 \leq material_{p\text{-}type} \leq 27$ where $material_{p\text{-}type} \in \mathbb{Z}$

$1 \leq N \leq 10000$

$0 \leq U \leq 100$

As a population-based approach, NSGA-II is well suited to this multiobjective problem [54]. For this study, the size of the population at each generation was set to 90 designs, 10 times the number of design variables. The selection method is tournament with 4 candidates, and the crossover operator is scattered with 0.5 crossover rate. The mutation operator is uniform with a 5% chance of mutation. The algorithm terminated after 100 generations, and a hypercube was observed to ensure that the solutions converged.

4.3. Single Objective Optimization

In addition to the multiobjective optimization, single objective optimization exploring different objectives and aimed towards maximizing or minimizing just one performance outcome is also used in this study. The multiobjective optimization is used to observe general

trends of the design variables and to explore performance characteristics and limits of the two different device architectures.

To work towards a more detailed analysis, single objective problems breaking down H into operating cost and capital cost will be explored. Both a genetic algorithm and simulated annealing approach are used. From the multiobjective optimization results that will be introduced in Chapter 5, it is observed that the BiSbTE nanobulk for the bulk device and PEDOT material for the hybrid device dominate the design space as both a low cost and high performing material selection. Thus p-type and n-type material choice are removed as a design variable, so design variables considered are the thickness of the TE leg (t), width of the TE leg (w), length of the TE leg (L), the space between the legs (δ), input current (I), p-type material, n-type material, the number of thermocouples (N), and the overall heat transfer coefficient of the heat exchanger (U). The side constraints given for each of these design variables in Eq. (4.3) and (4.4) will also be used in the single objective problems. First, the minimum device area required to produce a given cooling capacity will be studied. Then, the incorporation of the cost metric will be examined to determine the effects of considering cost on the design of a TEC system. The minimization of two cost goals, minimizing capital cost and minimizing operating costs, are analyzed.

The genetic algorithm function in MATLAB and a basic simulated annealing code with the ability to handle constraints are used to solve for optimal solutions [55],[56]. The genetic algorithm default settings in MATLAB are used with the exception of setting the population size to 10 times the number of design variables [55]. In simulated annealing, the

cooling is simulated by a temperature parameter (T) and is controlled using Boltzmann's probability distribution, given in Eq. (4.5).

$$P(E) = e^{-E/kT} \tag{4.5}$$

In this equation, E is the energy level, k is Boltzmann's constant, and $P(E)$ denotes the probability of reaching energy level E. For a set of design variables $\boldsymbol{x}_i$, the energy level E_i equals $f(\boldsymbol{x}_i)$. A new design point ($\boldsymbol{x}_{i+1}$) is generated and the change in energy states if given by Eq. (4.6) and the Boltzmann probability is updated using Eq. (4.7).

$$\Delta E = E_{i+1} - E_i = f(x_{i+1} - x_i) \tag{4.6}$$

$$P(E_{i+1}) = \min\{1, e^{-\Delta E/kT}\} \tag{4.7}$$

If $\Delta E \leq 0$, indicating an improvement in the objective function, then $P(E_{i+1}) = 1$ and the new design is accepted. The temperature is then reduced by the temperature reduction factor, and another iteration is performed until a final temperature is reached. In this study, initial temperature is set to 1, and the final temperature is set to 1×10^{-10}. The Boltzmann constant (k) is 1, and temperature reduction is 0.8. For the simulated annealing code, a penalty function is used to handle constraints.

4.3.1. Minimize Device Area for a Given Cooling Capacity

When beginning this study, it is believed that the hybrid device will require a larger number of thermocouples and a much larger area to produce the same amount of cooling when compared to a bulk device. This belief is based on the geometric differences of the two architectures: a leg of the hybrid device occupies a larger footprint than a bulk TEC leg, resulting in less thermocouples for a given area and thus less heat flux per given area. It is unknown how much larger the device will need to be, so it is difficult to determine bounds on

the number of thermocouples and constraints on the area of the device for given applications. To help determine the differences in area requirements for the bulk and the hybrid architectures, a single objective optimization problem is formulated to minimize the cross-sectional area of a device for a given Q_C. This allows for a reference to use when considering applications of TECs where the cooling capacity, desired operating temperatures, and allowable cross-sectional area of the TEC are known. Eq. (4.8) and (4.9) provide the objective function and constraints that, along with the side constraints for t, w, L, δ, N, and U, define the optimization problem. The objective is to minimize cross-sectional area of the device with two inequality constraints to maintain the Q_C within plus or minus 5% of a target Q_C value (y) and side constraints on the design variables.

$$\text{Minimize:} \quad f = \mathrm{A_{total}} = \mathrm{AN} \tag{4.8}$$

$$\text{Subject to:} \quad Q_\mathrm{C} - 1.05y \le 0$$

$$0.95y - Q_\mathrm{C} \le 0$$

$$0.5 \text{ mm} \le t \le 0.8 \text{ mm}$$

$$0.5 \text{ mm} \le w \le 0.8 \text{ mm}$$

$$0.1 \text{ mm} \le L \le 1 \text{ mm}$$

$$0.1\text{mm} \le \delta \le 2 \text{ mm}$$

$$0.1 \text{ A} \le I \le 10 \text{ A}$$

$$1 \le N \le 100000$$

$$0 \le U \le 100$$

Minimize: $f = A_{total} = AN$ (4.9)

Subject to: $Q_C - 1.05y \leq 0$

$0.95y - Q_C \leq 0$

$50\ \mu m \leq t \leq 250\ \mu m$

$10\ mm \leq w \leq 20\ mm$

$10\ mm \leq L \leq 20\ mm$

$0.1 mm \leq \delta \leq 2\ mm$

$0.1\ A \leq I \leq 10\ A$

$1 \leq N \leq 100000$

$0 \leq U \leq 100$

4.3.2. Minimize Capital Cost for a Given Cooling Capacity

In some design situations, the goal of the designer may be to minimize the capital cost of a TEC. In previous design optimization research on TECs presented in [36] and [17], just the cost of TE material was considered to determine device cost, making the cost dependent only on the volume of the material used. When incorporating the cost of a heat exchanger, it may be thought that minimizing the device area will minimize the cost of a heat exchanger. However, as the area of a device increases it may be possible to complete remove the heat exchanger while producing a given heat transfer rate. This is demonstrated by Eq. (4.10), which is commonly used to describe the heat transfer between two streams in a heat exchanger.

$$Q = UA\Delta T \tag{4.10}$$

In this equation, Q is the heat transfer rate, U is the overall heat transfer coefficient, A is the heat transfer surface area, and ΔT is the temperature difference between the two streams. As the area of the device increases, a smaller overall heat transfer coefficient can be used to produce a desired heat transfer rate. By adjusting U as a design variable and varying A by the inclusion of device geometries as design variables, the heat exchanger characteristics can be modeled and an appropriate heat exchanger can be selected based on the quantity UA. Calculations can be performed to determine when natural convection is adequate to produce a desired heat transfer rate, but these equations are dependent on the orientation of the device in space. By incorporating heat exchanger and substrate costs a designer can get more information on the overall system cost of a TEC. The formal problem statements to minimize the capital cost (defined in Eq. (3.18)) are given by Eq. (4.11) and (4.12).

$$\text{Minimize:} \quad f = C_{capital} \tag{4.11}$$

$$\text{Subject to:} \quad Q_C - 1.05y \leq 0$$

$$0.95y - Q_C \leq 0$$

$$0.5 \text{ mm} \leq t \leq 0.8 \text{ mm}$$

$$0.5 \text{ mm} \leq w \leq 0.8 \text{ mm}$$

$$0.1 \text{ mm} \leq L \leq 1 \text{ mm}$$

$$0.1\text{mm} \leq \delta \leq 2 \text{ mm}$$

$$0.1 \text{ A} \leq I \leq 10 \text{ A}$$

$$1 \leq N \leq 100000$$

$$0 \leq U \leq 100$$

Minimize: $f = C_{capital}$ (4.12)

Subject to: $Q_C - 1.05y \leq 0$

$0.95y - Q_C \leq 0$

$50\ \mu m \leq t \leq 250\ \mu m$

$10\ mm \leq w \leq 20\ mm$

$10\ mm \leq L \leq 20\ mm$

$0.1 mm \leq \delta \leq 2\ mm$

$0.1\ A \leq I \leq 10\ A$

$1 \leq N \leq 100000$

$0 \leq U \leq 100$

4.3.3. Minimize Operating Cost

The low efficiency of TECs has been a major disadvantage and has limited their adoption to only niche applications. To improve the efficiency of a device and achieve lower long-term costs, a designer may wish to minimize the operating cost of a TEC. To reach a lower operating cost, the device must have a large *COP*. However, this may sacrifice the capital cost of the device by increasing the complexity of the heat exchanger or inflating the size of the TEC. As a result, it is necessary to explore which devices require minimal operating costs. The formal problem statement to minimize the operating cost of a TEC for a defined Q_C is given in Eq. (4.13) and (4.14) for the bulk and hybrid devices. Once again, Q_C is maintained within plus or minus 5% of a target Q_C value (y). Additionally, various

constraints, designated by the value z, on the cross-sectional area of the device (A_{total}) are explored.

Minimize: $f = C_{operating}$ (4.13)

Subject to: $Q_C - 1.05y \leq 0$

$0.95y - Q_C \leq 0$

$A_{total} - z \leq 0$

$0.5 \text{ mm} \leq t \leq 0.8 \text{ mm}$

$0.5 \text{ mm} \leq w \leq 0.8 \text{ mm}$

$0.1 \text{ mm} \leq L \leq 1 \text{ mm}$

$0.1\text{mm} \leq \delta \leq 2 \text{ mm}$

$0.1 \text{ A} \leq I \leq 10 \text{ A}$

$1 \leq N \leq 100000$

$0 \leq U \leq 100$

Minimize: $f = C_{operating}$ (4.14)

Subject to: $Q_C - 1.05y \leq 0$

$0.95y - Q_C \leq 0$

$A_{total} - x \leq 0$

$50 \text{ μm} \leq t \leq 250 \text{ μm}$

$10 \text{ mm} \leq w \leq 20 \text{ mm}$

$10 \text{ mm} \leq L \leq 20 \text{ mm}$

$0.1\text{mm} \leq \delta \leq 2 \text{ mm}$

$$0.1 \text{ A} \leq I \leq 10 \text{ A}$$

$$1 \leq N \leq 100000$$

$$0 \leq U \leq 100$$

4.4. Summary

Using optimization and considering the operating and capital costs of a TEC, a designer can make better and more informed decisions about selecting a TEC for an application. The multiobjective problem to maximize cooling capacity and minimize cost simultaneously and the three single objective optimizations are just a few problems that can help designers understand the advantages and disadvantages of the hybrid and bulk architectures. When the designer is equipped with specifications, including the required cooling capacity, operating temperatures, and area constraints, these single objective problems to minimize area, minimize capital cost, and minimize operating cost incorporate important considerations in the construction of a TEC. Furthermore, to find suitable real world applications, it is necessary to consider the implications of the insights gained through design optimization. With this in mind, the next chapter presents the results for each of the optimization scenarios and then works towards bridging the gap between the theoretical and real world applications by considering a simplified design scenario to demonstrate how the insights gained through design optimization can be used in an actual design problem.

5. RESULTS AND DISCUSSION

Design optimization is an important tool in gaining a better understanding of both the performance and design spaces of a system. The information gained through different optimization problems and their results can help provide insight into how the bulk and hybrid architectures perform and the trade-offs between cost of the TEC system and cooling performance. Additionally, the inclusion of multiple design variables can give insight on the geometric factors, TE materials, heat exchanger components, and operating current of an entire TEC system. The results from the optimization problems described in Chapter 4 are given here and discussed to gain a deeper understanding of a TEC system and its associated costs. In additional, a case study of a compact refrigerator is presented to begin working towards application and provide context to the design optimization problems presented in this study.

5.1. Multiobjective Optimization

Pareto frontiers were generated according to the problem statements given in Eq. (4.3) and (4.4). NSGA-II was used to perform the optimization to produce a set of Pareto optimal solutions, the feasible designs where no other solutions exist in which simultaneous improvement in all objectives can occur. The two objectives are to minimize total system cost (H) and maximize cooling capacity (Q_C) while considering several design variables. A Pareto optimal solution represents a trade-off between the two objectives, meaning cost cannot be reduced any further without also reducing the cooling capacity. Likewise, a design on the frontier cannot improve its cooling capacity without increasing the cost of the device. As mentioned in Chapter 4, the design variables considered are:

- thickness of the TE leg (t),
- width of the TE leg (w),
- length of the TE leg (L),
- space between the legs (δ),
- input current (I),
- p-type material ($material_{p\text{-}type}$),
- n-type material ($material_{n\text{-}type}$),
- number of thermocouples (N),
- and, the overall heat transfer coefficient of the heat exchanger (U).

5.1.1. Performance Space

To reach a preliminary understanding of the performance space, the Pareto optimal solutions are shown in Figure 5.1 for the bulk and hybrid devices. The hybrid device solutions are under 300 W of cooling capacity while the bulk devices are able to produce much larger cooling capacities. This can be attributed not only to the variation in geometric factors between the bulk and hybrid architectures but also the lower ZT values of TE materials available for printing on the PET substrate. The range of costs are similar for both the hybrid and bulk. Initial expectations are that the hybrid device would be most effective in low density cooling applications. As indicated in the colorbar on Figure 5.1, the results from the optimization confirm this as the hybrid device produces cooling densities lower than the bulk device. The bulk device achieves a heat flux exceeding 14,000 W/m^2 while the hybrid device remains below 2000 W/m^2.

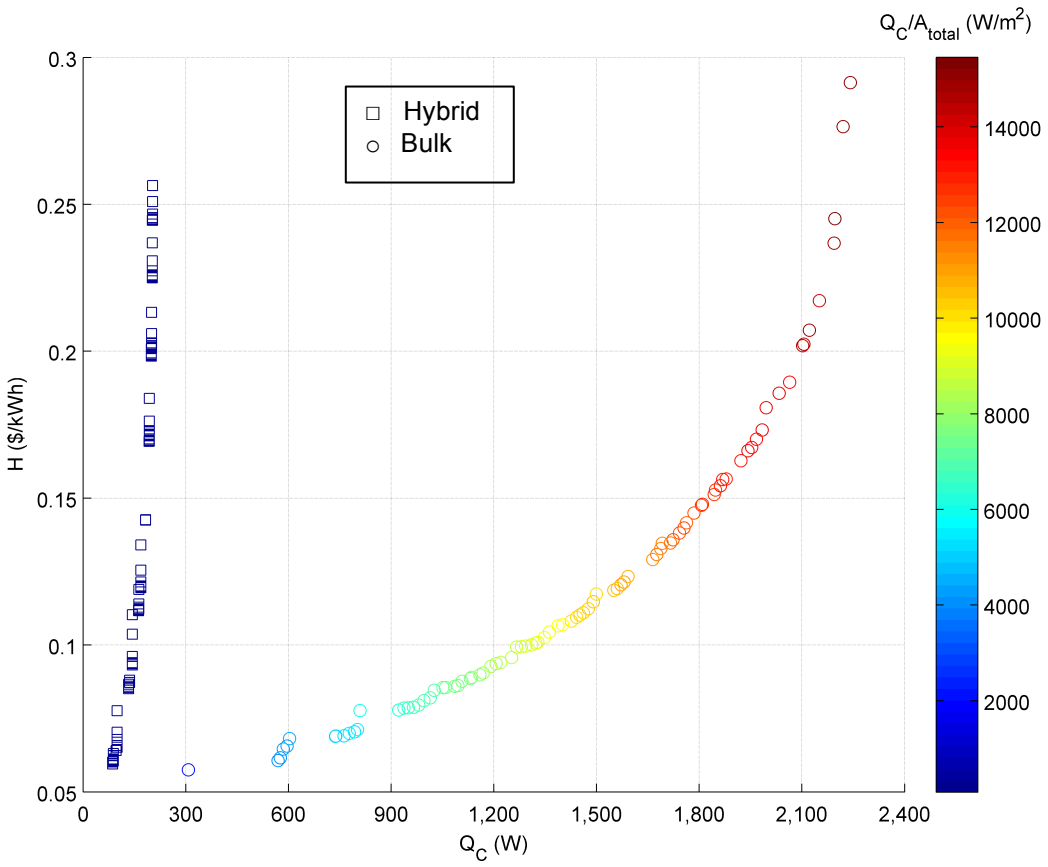

Figure 5.1. Pareto Frontiers for Maximum Cooling Capacity and Minimum Cost

As context to the values generated, the heat flux of R134a direct expansion evaporator coils used in air conditioning and refrigeration can range from 6000-8500 W/m^2, and an Energy Star rated central air conditioning unit must have a *COP* greater than 3.22, which translates to an operating cost of \$0.0321/kWh [57]. Ongoing research is exploring the use of TECs in high heat flux (>100,000 W/m^2) applications like actively cooling electronic devices, but current designs have *COP*s less than 1 (operating cost calculated by C_e divided by *COP* would be greater than \$0.1035/kWh) [58]. As additional references, it is noted that

a standard compact refrigerator produces 30-45 W of cooling, and a window unit air conditioner outputs approximately 1500 W of cooling capacity [59], [60].

5.1.2. Design Space

The set of plots in Figure 5.2 colors the bulk device Pareto frontier according to design variable values. Likewise, the set in Figure 5.3 deliniate the hybrid design variable values across the Pareto frontier. Every optimal design populating the frontier from the hybrid architecture had the polymer (PEDOT) material choice, and every optimal design from the bulk architecture optimization used the BiSbTe nanobulk material. This is analagous to the results seen in LeBlanc et. al's study where the BiSbTe nanobulk material (identified as having nanoscale grain structures) performs well on a $/kWh basis [15]. When calculating a *ZT* per dollar for each of these materials, PEDOT has the highest efficiency per dollar for the hybrid material choices, and BiSbTe nanobulk presents the best efficiency per dollar for the bulk material choices. Another important observation is differences between the overall heat transfer coefficient (U) for both architectures. Since the area of the hybrid devices are very large, a heat exchanger with a lower heat transfer coefficient can be used to produce a cooling rate across the exchanger, and the heat exchanger component can be greatly simplified. The last observation noted is the optimal current input. As cooling density increases across the Pareto frontier (i.e. more cooling per unit area), the input current increases. A larger current linearly increases the heat pumping capacity of the cooler, but if too large, joule heating, which is dependent on I^2, can reverse the cooling effects of the device.

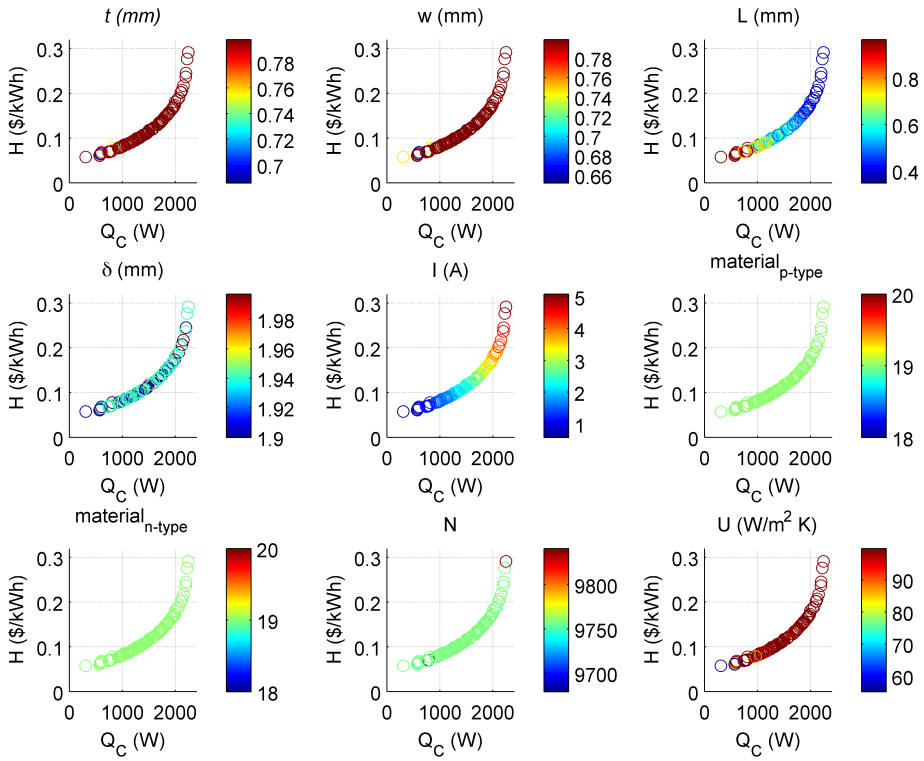

Figure 5.2. Trends in Design Variables for Bulk Architecture

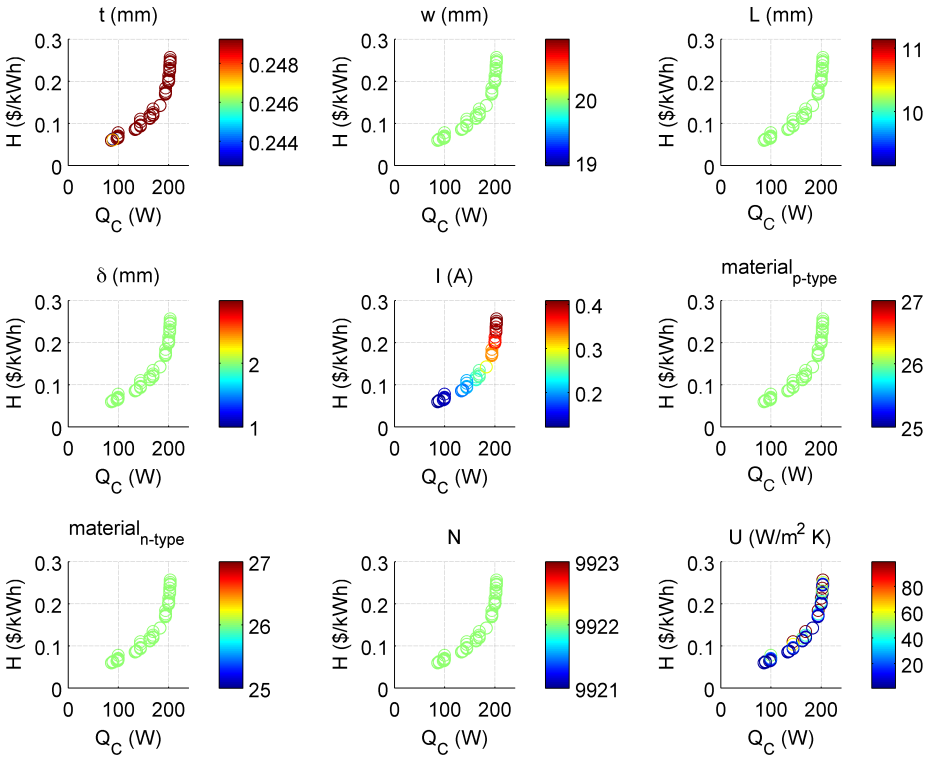

Figure 5.3. Trends in Design Variables for Hybrid Architecture

For both architectures, each Pareto optimal solution pushed towards the upper bound on thickness (*t*) and width (*w*) to make the TE legs as wide as possible. An important factor in the design of a TEC is the ratio of leg cross-sectional area to leg length. In the bulk optimization, the leg area stays constant while the length changes to alter the ratio between the two. A larger ratio translates to increased thermal and electrical conductivity, and a smaller ratio means decreased thermal and electrical conductivity. As discussed previously with materials, this presents a trade-off in efficiency and performance capabilities of the device. A large thermal conductivity limits the devices ability to maintain a temperature difference, and a large electrical conductivity lessens the effects of Joule heating. It is

commonly observed that the as the requirement for Q_C increases, the leg length shortens. This same effect is not observed in the optimization of the hybrid device, where the leg length remains at the lower bound. The ratios from the bulk optimization range from approximately 0.8 to 1.6. With the leg areas of the hybrid device at their largest and leg length at its shortest value, the largest possible ratio is 0.5. To produce more cooling, a larger ratio is required, but the hybrid architecture is limited by the bounds on the leg thickness, width, and length design variables. Further study and prototyping of a device is need to test the manufacturing limits of these variables and to assess improvements in design.

5.1.3. Identifying Future TEC Improvements

The results in this section work towards the second research question. Details in Chapter 2.1 provide information on the attributes of thermoelectric materials. To increase the thermoelectric figure of merit (ZT), three goals are outlined: increase the Seebeck coefficient (α), decrease thermal conductivity (κ), and increase electrical conductivity (ρ). Table 5.1 shows the material properties of the optimal material (BiSbTe nanobulk) from the previous section, BiTe (common material selection for current commercially available TECs), and each property if BiSbTe were improved by different percentages for each TE material property (e.g. increase α by 10%, decrease κ by 10%) without adding any additional cost. The same multiobjective optimization as described for the last section is performed with one exception: limiting the material choice to those outlined in Table 5.1. Results are depicted in Figure 5.4.

Table 5.1. Improved Material Properties for Analysis

Material	α (V/K)	ρ (ohm mm)	κ (W/mm-K)	ZT(300 K)
BiTe	0.000227	0.011475	0.00157	0.858
BiSbTe Nanobulk	0.000224	0.013177	0.00068	1.680
10% Improvement	0.000246	0.014495	0.00061	2.053
20% Improvement	0.000269	0.015812	0.00054	2.520
30% Improvement	0.000291	0.017130	0.00048	3.120

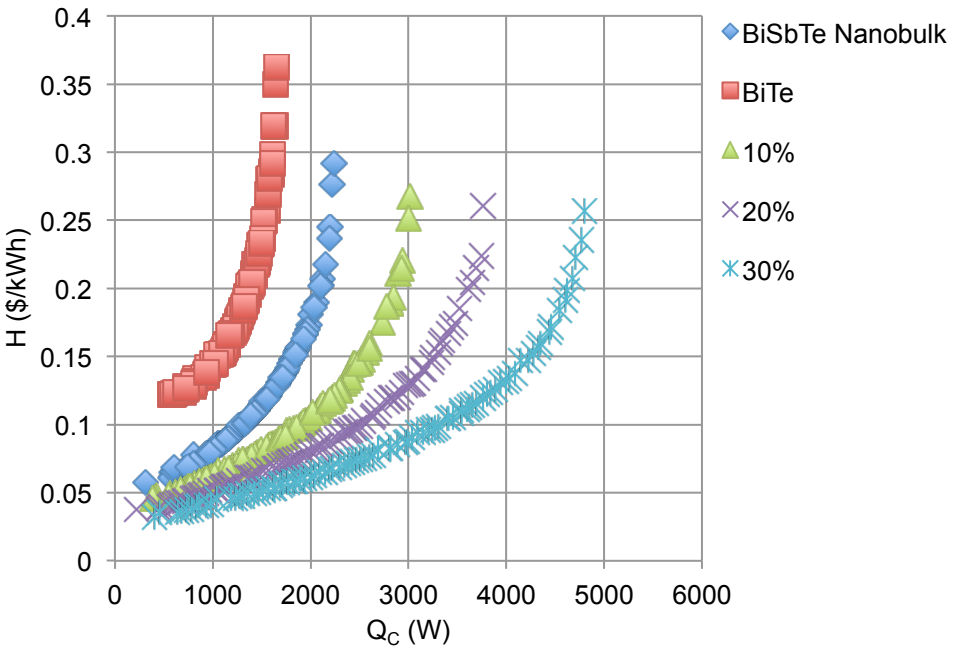

Figure 5.4. Pareto Frontiers for Improved Hypothetical TE Materials in a Bulk TEC

These results indicate the potential of TE material technology. Commercially available TECs use BiTe as the thermoelectric material [3]. A Pareto frontier for the case limited by material choice to the commonly used BiTe semiconductor provides a baseline for

measuring performance improvements. By including the TE material type as a design variable and analyzing improvements to *ZT* values, significant performance improvements are seen. Additionally, *COP* increases with improvements in *ZT* value. This also corresponds to an improvement in operating costs. As *ZT* of the improved material approaches 3.12, *COP* values of the bulk TEC reach 3.14, which is more comparable to traditional methods of refrigeration. As a reference, an Energy Star rated central air conditioning unit must have a *COP* greater than 3.22 [57]. Table 5.2 provides the minimum, maximum, and median values from the Pareto optimal solutions.

Table 5.2. *COP* Results for Pareto Optimal Solutions

Material	**Minimum *COP***	**Maximum *COP***	**Median *COP***
BiTe	0.276	0.826	0.567
BiSbTe Nanobulk	0.343	1.762	0.927
10% Improvement	0.374	2.203	1.133
20% Improvement	0.384	2.656	1.252
30% Improvement	0.390	3.141	1.261

The polymer hybrid device performs poorly in both objectives when compared to the alternative bulk devices. Printable TE materials that are currently available for application are limiting the performance of the hybrid device. To identify the potential of the hybrid architecture if printable technologies improved in efficiency, a frontier limiting the material choice to BiSbTe nanobulk for a hybrid device is shown in Figure 5.5. It is important to note

that while the BiSbTe on the hybrid device greatly improves the performance, the heat flux is still much lower than the bulk device with the same material. The median cooling capacity per area (Q_C/A) for all the designs on the Pareto frontier for the BiSbTe hybrid device is 1808.6 W/m^2; in contrast, the median value of the BiSbTe bulk frontier is 10,011.1 W/m^2.

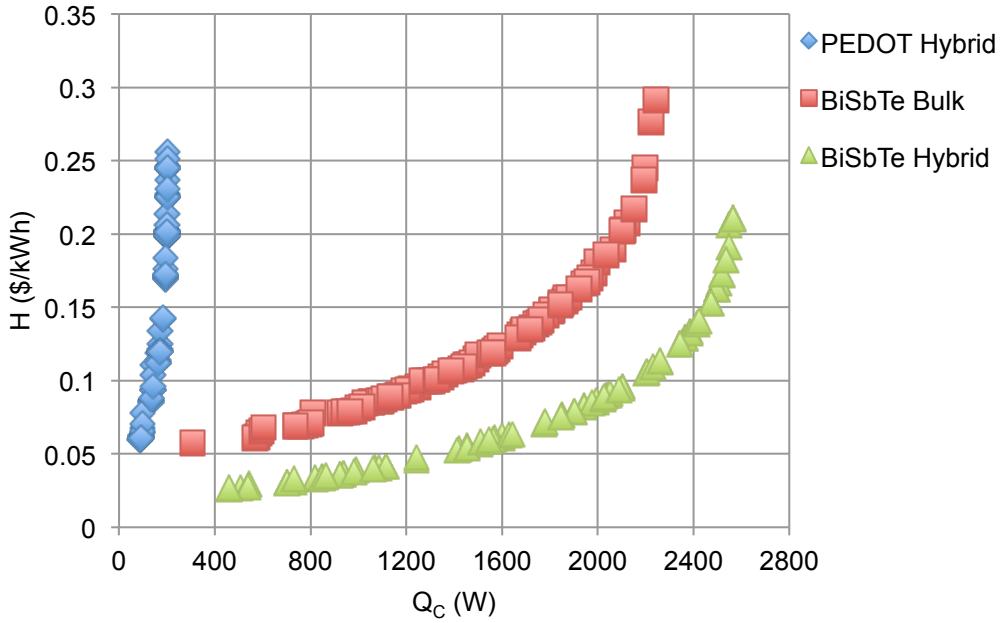

Figure 5.5. Pareto Frontier Using Bulk Materials for the Hybrid Architecture

5.2. Single Objective Optimization

Several different performance objectives are explored using single objective optimization. The first is to minimize the cross-section device area. Both SA and GAs are analyzed for this problem. Secondly, two objectives involving cost are analyzed: minimize overall system cost and minimize operating cost.

5.2.1. Minimize Device Area for a Given Cooling Capacity

The goal of the optimization algorithm discussed in this section is to minimize the cross-sectional area of a device (A_{total}) while achieving a target cooling capacity (Q_C). The problem formulation is given in Eq. (4.8). For target Q_C values ranging from 10 to 1000 W, both SA and GA are used to minimize Q_C in intervals of 10 W. The results for the bulk and hybrid architectures are shown in Figure 5.6 and Figure 5.7, respectively. Both SA and GA approaches are demonstrated. On average, one run of SA evaluated 54,412 designs for the bulk device and 52,687 for the hybrid architecture to solve for the optimal area of a TEC. In contrast, the GA evaluated approximately 4,600 designs each run. The SA more consistently arrived at a global optimum, appearing to be a more robust approach to this problem. However, the computational burden of evaluating ten times more designs is a major disadvantage of using simulated annealing. It is observed from the results that while the GA settles on local optimum, the GA finds the optimal solution in a much more reasonable time period than SA and still provides information on trends and results in both the performance and objective spaces.

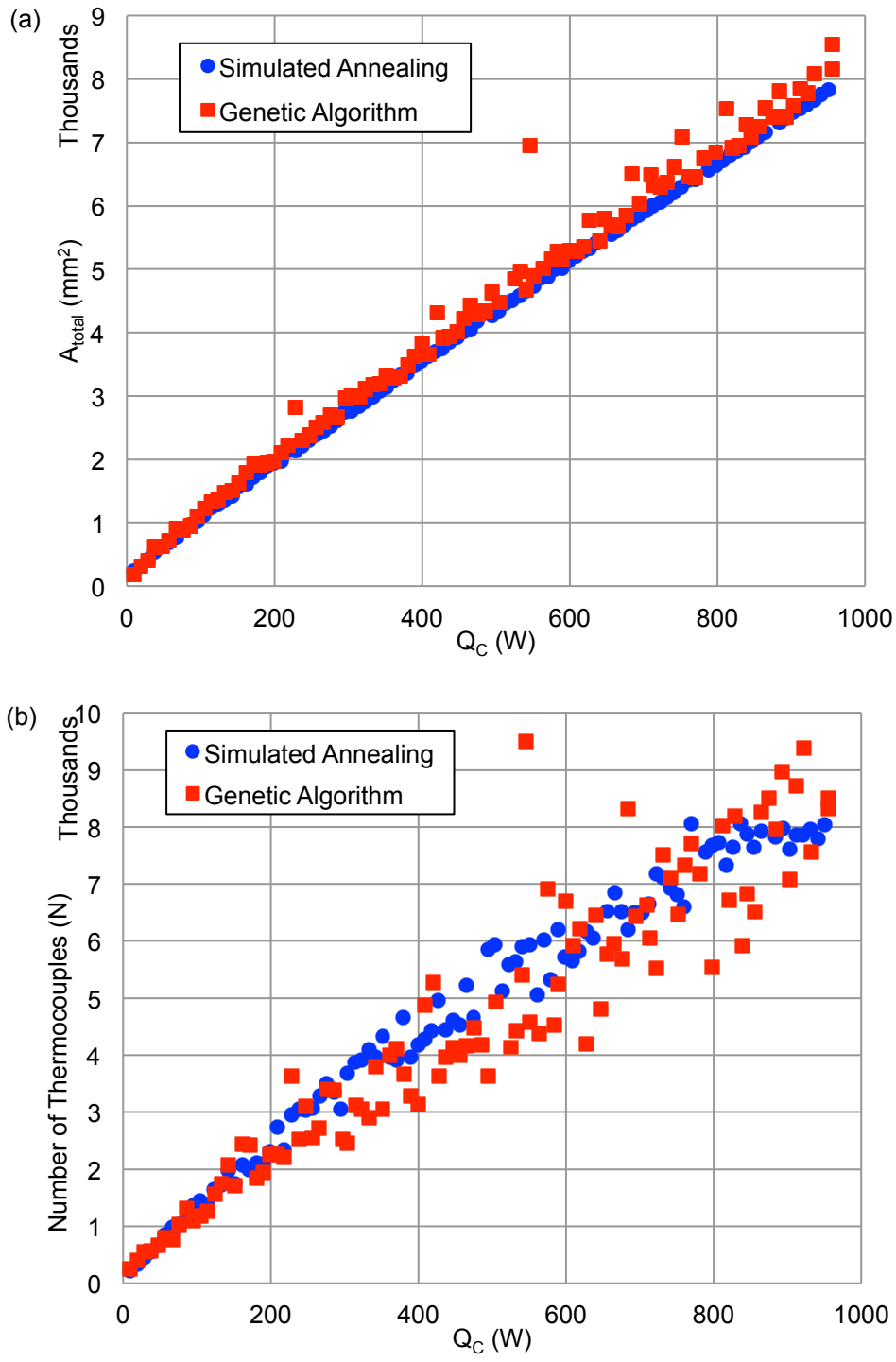

Figure 5.6. (a) Minimum Cross-Sectional Area to Produce a Given Q_C and (b) Corresponding Number of Thermocouples of the Bulk Architecture

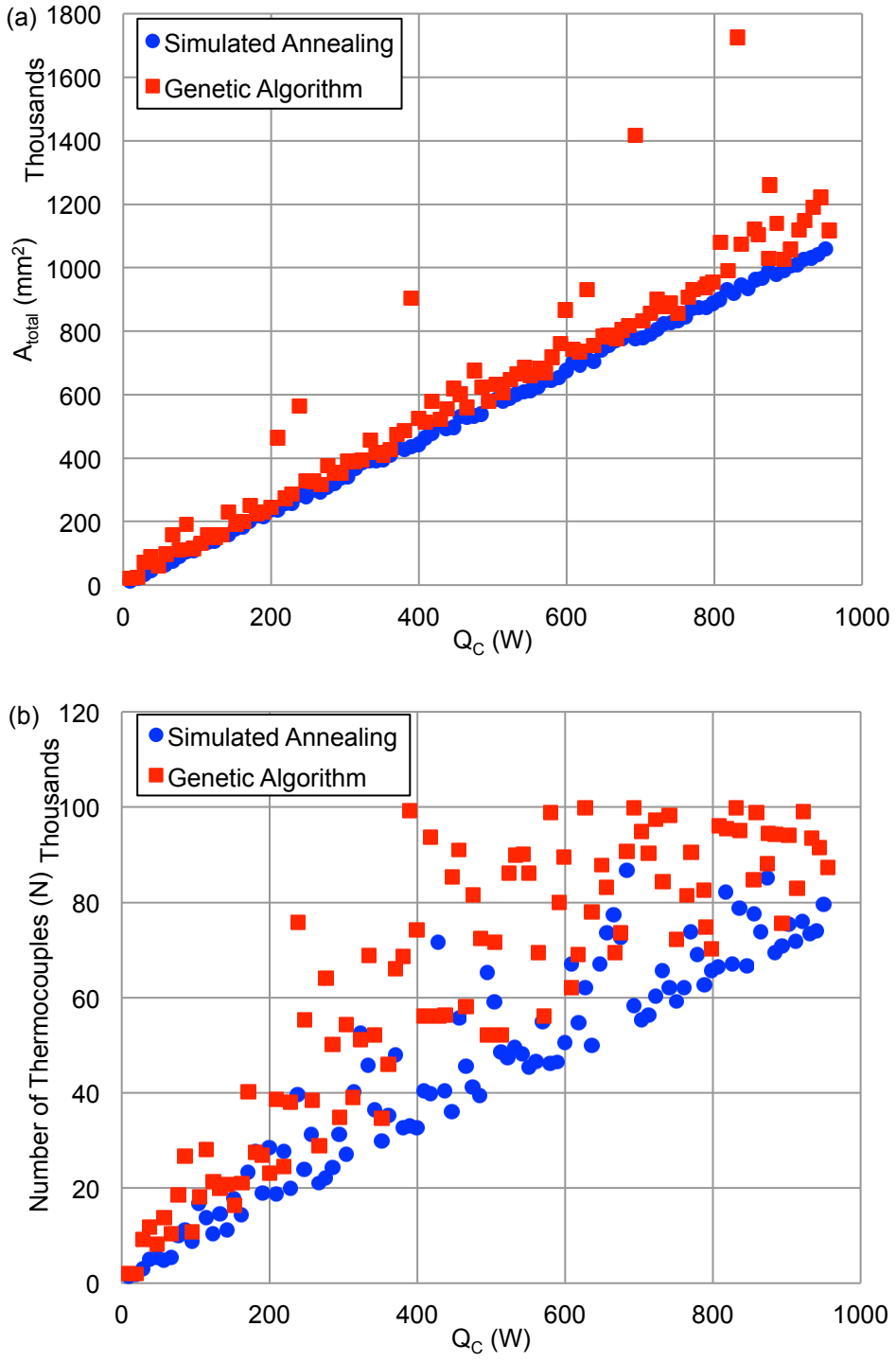

Figure 5.7. (a) Minimum Cross-Sectional Area to Produce a Given Q_C and (b) Corresponding Number of Thermocouples of the Hybrid Architecture

From these results, it is evident that a hybrid device requires a much larger area than the bulk device to produce a required cooling capacity. However, the number of thermocouples (N) needed is only approximately 10 times more for the hybrid device when compared to a bulk. N follows a general linear trend as requirement for cooling and device area increase; while there is variability in the number of thermocouples that deviate from a linear trend, this is attributed to variability in the other design variables affecting device geometry. This translates into a much larger area to produce a cooling capacity. This is due to the bounds on the design variables defined by manufacturing considerations and the efficiency of the materials. As defined by the side constraints on the design variables, the largest possible area for a bulk TE leg is 0.64 mm^2 (0.8 mm thick by 0.8 mm wide) opposed to 5 mm^2 (0.25 mm thick by 20 mm wide) for a hybrid TE leg. When including the maximum allowable spacing between the legs, one thermocouple of a bulk device has a cross-sectional area up to 15.68 mm^2, and the hybrid device has a cross-sectional area up to 99 mm^2. In addition, the ZT of PEDOT material of the hybrid TEC in each of the designs is only 0.26, while the nanobulk material BiSbTe used in the bulk devices has a ZT of 1.68. These two characteristics of the hybrid device necessitate the larger area to produce a required cooling rate.

The implications of the large area requirements of the hybrid TEC may limit the feasible implementations of the device but also suggest possibilities for niche applications. For example, if a designer is selecting a TEC for an application that has a thermal load of 200 W to cool an object from 20°C to 0°C, the minimum size required for the hybrid architecture is approximately 245,500 mm^2 (0.2455 m^2). As context, a standard 8 quart catering chafing

dish has a surface area of approximately 0.281 m^2 [61]. The bulk device only requires approximately 2000 mm^2, two orders of magnitude smaller than the hybrid TEC. To produce 900 W, the minimum hybrid device size is approximately 1,000,000 mm^2 (1 m^2) opposed to approximately 7000 mm^2 for the bulk TEC. However, these large area requirements may prove advantageous in certain applications where a large heat transfer area is beneficial. An example of a low heat flux application is personalized cooling and heating, such as an office chair embedded with TECs. In these low heat flux uses, localized spot cooling, as with a computer chip releasing a large amount of heat in a small area, is not needed.

5.2.2. Minimize Capital Cost

An important design consideration is the capital cost of a TEC. The results here are for the optimization problem to minimize capital cost for a given cooling capacity. Only a GA approach is used to solve for the optimal solution as results indicated in the previous section that while sometimes settling on local optimum, the GA is able to quickly and efficiently achieve results in this problem. Figure 5.8 indicates the results for both device architectures and resultant characteristics of the optimal design, including the operating cost, number of thermocouples, and heat exchanger characteristics. These three characteristics, in addition to the area of the device, encompass the major components of the total system costs. Consistent with the previous section, it is evident that the hybrid device required many more thermocouples, and thus a much larger area, to produce a desired cooling capacity. In addition, due to this large area, the heat exchanger is simplified. The overall heat transfer coefficients of the hybrid devices are so low that natural convection can be used to dissipate heat on the hot side of the device, and no heat exchanger even needs to be added to the

system. The overall heat transfer coefficient times area is lower for the hybrid device, resulting in a lower heat exchanger cost, calculated by $C_{HX}UA$. The operating costs are congruent to typical *COP* values observed in the literature. The range of *COP* values is 0.296 to 0.713 for the bulk devices and 0.074 to 0.855 for the hybrid architecture.

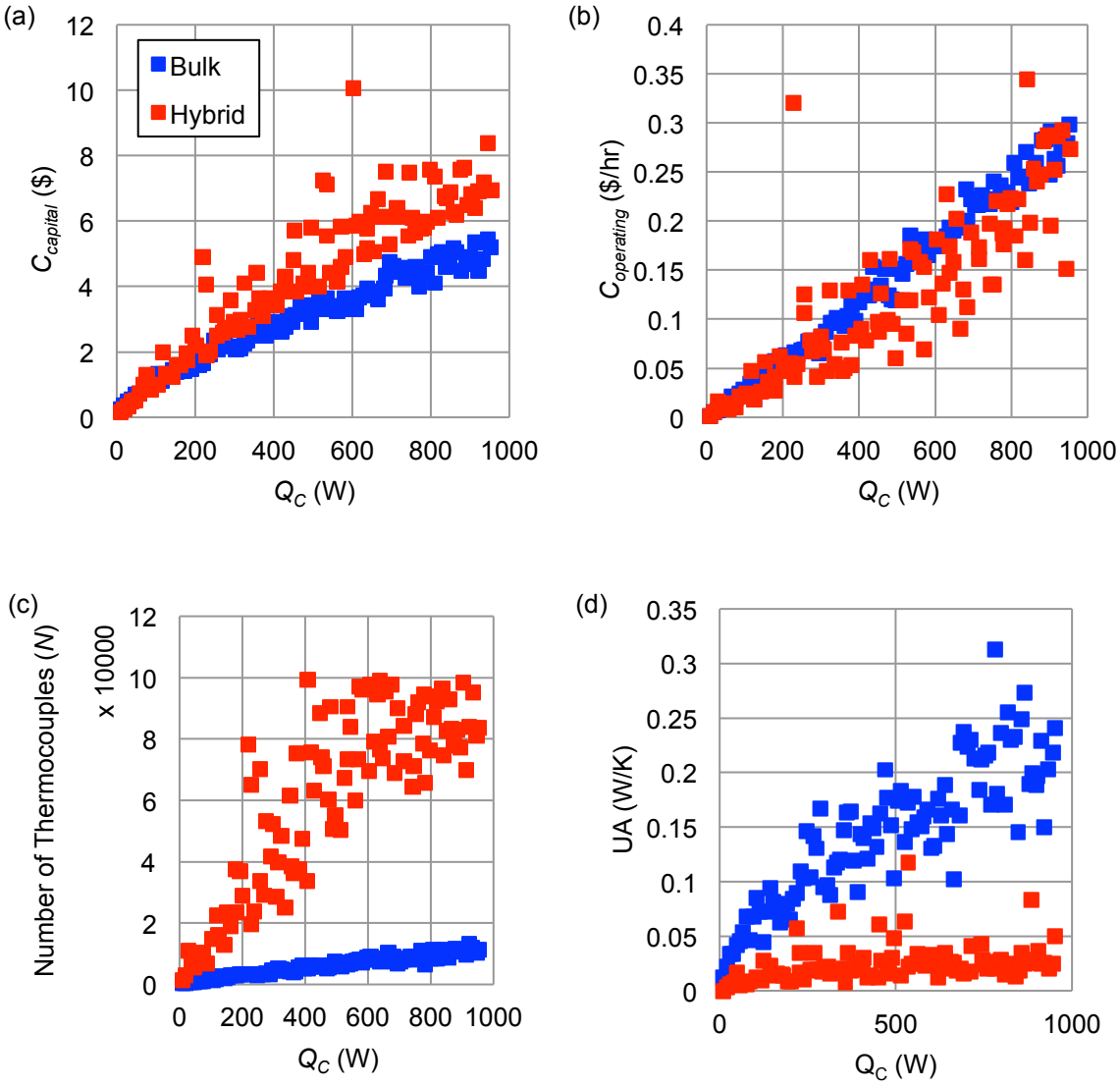

Figure 5.8. (a) Minimal Capital Cost at a Given Q_C for Bulk and Hybrid Architectures and the Resultant (b) Operating Cost, (c) Cross-Sectional Device Area, and (d) Heat Exchanger Characteristic

In addition to the number of thermocouples, other trends across the design variables are observed. The leg cross-sectional areas of the bulk device trend towards the lower bound for leg thickness and width to minimize the volume of material. Like the observations from the multiobjective optimization, the leg length decreased and input current increased as the cooling capacity requirement increased. Much more variation is observed for the leg geometries of the hybrid device, which may contribute to the variability in optimal solutions. The leg thickness and width varied while the length of the legs, as observed in the multiobjective optimization, pushed towards the lower bound. While this variation in design variable values is present, the designs tended to increase the ratio of leg area to length as cooling requirements increased. A trade-off between reducing the quantity of material and meeting the cooling requirements exists, as it is difficult for the hybrid device to achieve increased cooling capacities due to its low heat flux abilities while also reducing the cost associated to the TE material. The algorithm's ability to find more optimal designs could be hampered by this trade-off and thus settles on locally optimum solutions. The input current also increased as the cooling capacity requirement increased.

To further analyze the cost metric, the overall system cost ($C_{capital}$) is decomposed into the three major components: TE material cost, heat exchanger cost, and substrate cost. Figure 5.9 gives the breakdown of the capital cost for both architectures. Congruent with the increased U values of the bulk designs, the heat exchanger costs make up a greater percentage of the overall costs, averaging 37.2% of the total cost across each of the designs. In contrast, the heat exchanger costs only averaged 5.4% of the total costs for the hybrid designs. In detailed design, calculations can be performed that are dependent on the

orientation of the device and its operating environment in a specific application to determine if the heat exchanger is required or if natural convection is adequate to maintain the heat flow across the device. Additionally, the material cost constituted a large percentage of the hybrid architecture cost. While PEDOT is an inexpensive material and is easily manufactured via rotary screen printing and R2R processing, the number of thermocouples and volume of material required to produce large cooling capacities limits the economic attractiveness of the total system. Savings are seen regarding heat exchangers, but the large amount of TE material needed to make up for the material's inefficiency prohibits the minimization of costs. Lastly, for both architectures, the substrate costs were a small component of the total costs. Due to the large area of PET substrate required for the hybrid device, a greater cost is contributed by the hybrid substrate than for the bulk substrate. The consequences of these insights help to identify potential areas where the TEC systems can be improved. While the materials making up the hybrid device are inexpensive, the large volume of materials used inhibits savings in the total cost. The bulk system has a much larger heat exchanger costs, so savings from finding lower cost heat exchangers are an important consideration.

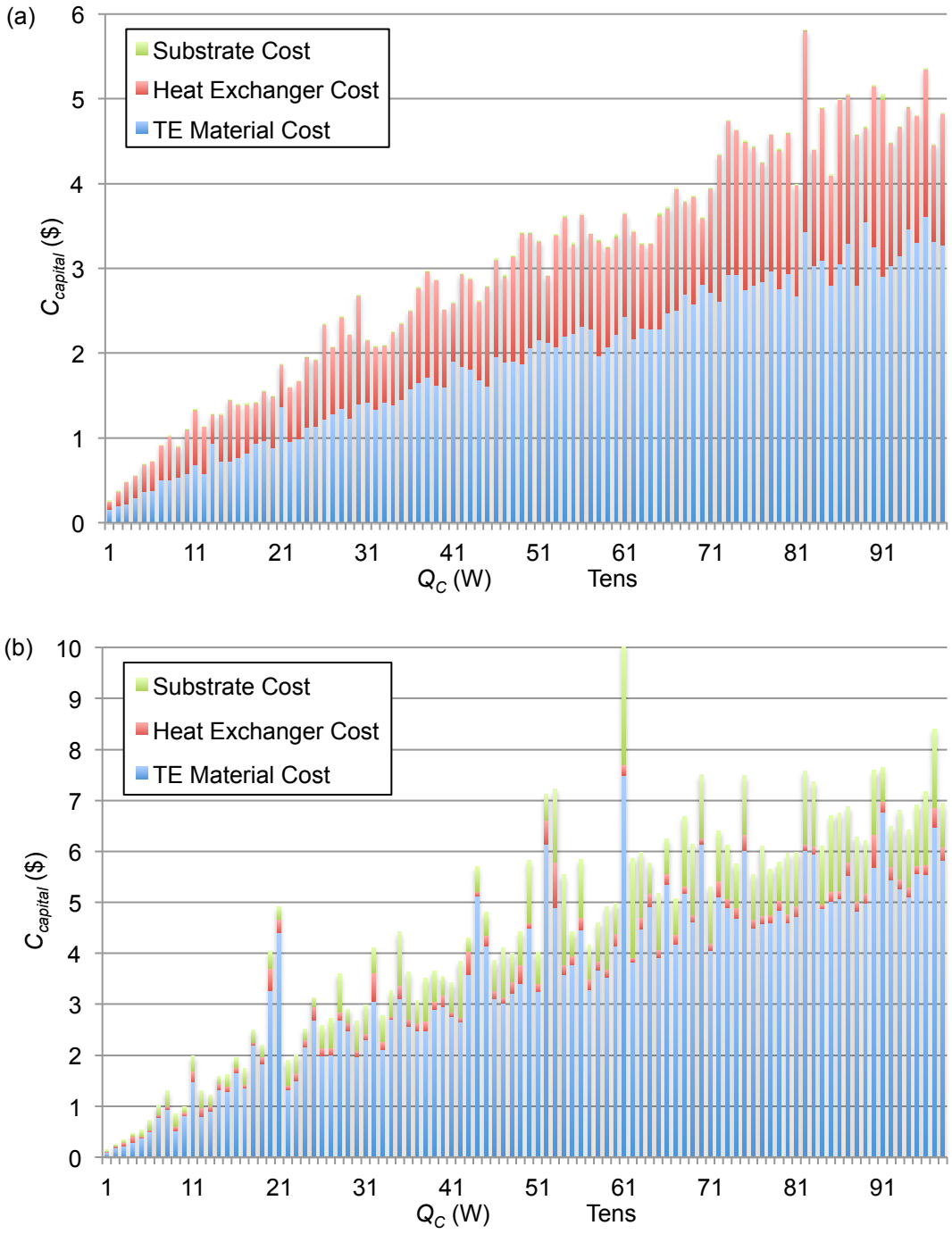

Figure 5.9. Breakdown of Capital Cost for (a) Bulk and (b) Hybrid Architectures

5.2.3. Minimize Operating Cost

Opposed to minimizing the capital costs of a TEC, a designer may wish to minimize the operating cost to reduce the lifetime expense of the device. In some applications, it might be important to limit A_{total}. In addition to an unconstrained optimization to find the minimum operating cost, four different constraints on A_{total} are examined: 500,000 mm^2 (0.5 m^2), 250,000 mm^2, 125,000 mm^2, and 62,500 mm^2. The results are shown in Figure 5.10. The bulk solutions range in area from 3,421 mm^2 to 60,004 mm^2. When unconstrained, the operating costs are reduced to under \$0.06/hr at 1000 W of cooling. This sharply contrasts the operating costs when minimizing for capital cost, which grew to as large as \$0.30/hr at 1000 W of cooling.

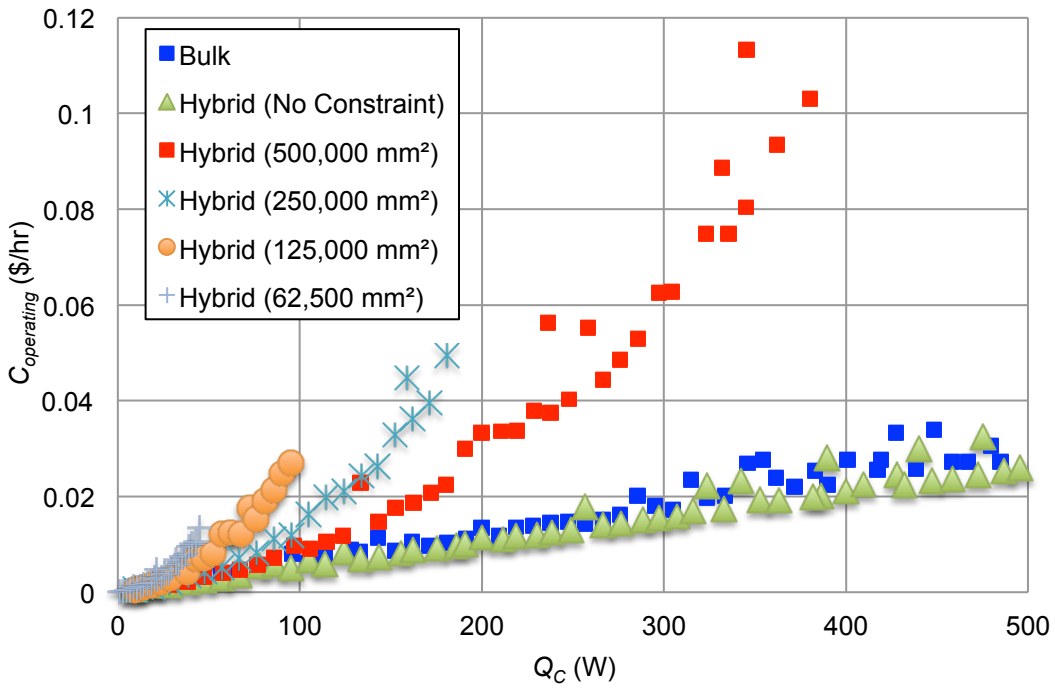

Figure 5.10. Minimized Operating Cost under Different Cross-Sectional Area Constraints

Table 5.3 gives the maximum and minimum *COP*s of the optimal solutions found for each scenario. The minimum *COP* corresponds to the maximum cooling capacity reached while the maximum *COP* corresponds to the minimum cooling capacity examined. As the constraints grow increasingly smaller and the constraint on area is approached, the cooling capacity output decreases and the operating costs of the hybrid device rapidly increase. This lends to a sharp rise in the operating cost of the device. When unconstrained, the hybrid device is competitive with the bulk design. As shown in the previous two sections, the area of the bulk device is minimal compared to the hybrid device; as a result, the operating cost of a bulk TEC is unaffected by the constraints explored here. Similar behavior would be expected if a constraint on A_{total} were small enough to effect the overall design of the system.

Table 5.3. Minimum and Maximum *COP* of Bulk and Hybrid TECs under Device Area Constraints

	Bulk		**Hybrid**	
Constraint	**Min *COP***	**Max *COP***	**Min *COP***	**Max *COP***
Unconstrained	1.242	1.791	1.126	1.932
500,000 mm^2	-	-	0.305	1.908
250,000 mm^2	-	-	0.356	1.827
125,000 mm^2	-	-	0.352	1.810
62,500 mm^2	-	-	0.335	1.891

When optimizing for operating cost instead of capital cost, the designs change with regard to two different design variables: input current and heat exchanger design. For the bulk device, current ranged between 1 A and 2.5 A when optimizing for capital cost, and under 1 A when optimizing for operating cost. A similar trend is observed with the hybrid device—input current ranged from 0.1 A and 0.3 A when optimizing for capital cost versus

0.1 A to 0.14 A when optimizing for operating cost. A In an actual application, the preferred current will most likely lie somewhere between that for optimal operating cost and for minimum capital cost. The heat exchanger characteristics also varied greatly between both optimization goals. To minimize capital costs, the heat exchanger is greatly simplified as it can be a major component of the overall system cost. When minimizing for operating costs, the overall heat transfer coefficient grows to increase the cooling transfer efficiency.

5.3. Working Towards Applications

In this section, a simplified design scenario is presented to indicate how the insights from design optimization can be used in real world problems. The scenario is to generate a design for a compact refrigerator. A commercially available vapor compression refrigerator by Frigidaire is used to develop a set of specifications, which are summarized in Table 5.4 [60]. The 2.4 ft^3 Frigidaire model has an annual energy consumption of 260 kWh, which translates to 29.7 W of power, and assuming a *COP* of 3.22 (based on Energy Star appliances), this refrigerator's cooling capacity is 95.6 W. The desired cold side temperature of 4°C is based on the Food and Drug Administration's recommended maximum food storage temperature, and the ambient temperature is decided by a worst case design scenario where the room the refrigerator is stored is at 27°C [62]. The size of the refrigerator dictates a constraint on area of the TEC. Assuming the shape is a cube and the TEC can only cover five surfaces of the cube, the maximum allowable TEC cross-sectional device area is 834,270 mm^2.

Table 5.4. List of Specifications for TEC Compact Refrigerator

Specification
Cooling Capacity will be between 95 W and 100 W
Maximum TEC device area is 834,270 mm^2
Cold side temperature (T_C) is maintained at 4°C
Ambient temperature (T_∞) is 27°C

Using a GA, the bulk and hybrid devices are optimized for total system cost (*H*). The same design variables and side constraints from the single objective problems discussed previously are used. As in Section 5.1.3, different TE materials (identified in Table 5.5) are explored to identify the potential of the bulk and hybrid TECs. 10%, 20%, and 30% improvements in BiSbTe material nanobulk properties are used in the optimization of the bulk device as well as 10%, 20%, and 30% improvements of the PEDOT material properties for the hybrid device. The results for each design under the different material selections are given in Figure 5.11.

Table 5.5. TE Materials Used in Design Scenario Optimization

Architecture Type	Material	α (V/K)	ρ (ohm mm)	κ (W/mm-K)	ZT
Bulk	BiTe	0.000227	0.011475	0.00157	0.858
	BiSbTe Nanobulk	0.000224	0.013177	0.00068	1.680
	10% Improvement	0.000246	0.014495	0.00061	2.053
	20% Improvement	0.000269	0.015812	0.00054	2.520
	30% Improvement	0.000291	0.017130	0.00048	3.120
Hybrid	PEDOT	0.00021	0.135135	0.00037	0.2646
	10% Improvement	0.000231	0.148649	0.00033	0.3234
	20% Improvement	0.000252	0.162162	0.00030	0.3969
	30% Improvement	0.000273	0.175676	0.00026	0.4914

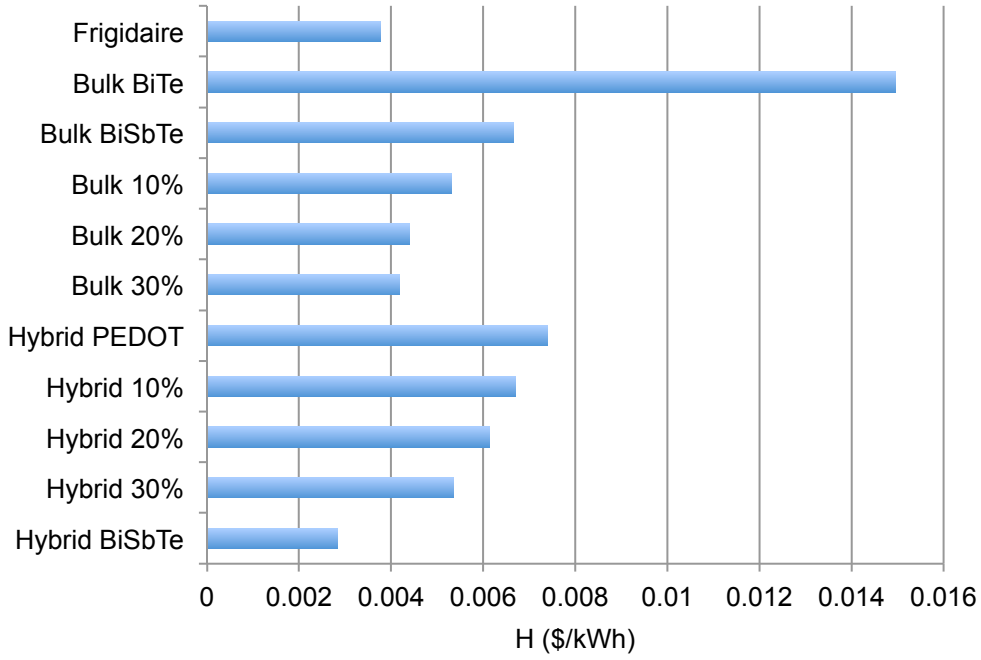

Figure 5.11. Total System Costs of Design Scenario TECs and Frigidaire Compact Refrigerator

Using the price of the refrigerator along with *COP*, the cost of the Frigidaire compact refrigerator is calculated according to Eq. (3.20). The only device costing less than the example design is a hybrid TEC with BiSbTe nanobulk as the thermoelectric material—this only demonstrates the potential of the hybrid TEC if printable TE materials with higher *ZT* values were available. As improvements in material efficiency are realized, TECs become a competitive alternative to traditional vapor compression refrigeration. It is important to note that the dominating component of the cost metric *H* is the operating cost, so when designing a TEC, consideration of *COP* and operating cost are integral in selecting a design.

Furthermore, the design variable values for each of these designs follow the trends presented with the multiobjective optimization. Cross-sectional areas are as large as possible, meaning the leg width and thickness approach the upper bounds of the side constraints. Leg length is as small as possible for the hybrid architecture while leg length of the bulk designs varies more. The optimal current is smaller for the hybrid device than for the bulk device, and the heat exchangers required for the hybrid devices are simplified or unnecessary. The overall cross-sectional areas of the devices were also much higher for the hybrid device. The bulk devices were all under 34,590 mm^2 (for the BiTe bulk TEC) while the smallest hybrid device was 222,054 mm^2 (for the hypothetical BiSbTe hybrid TEC).

5.4. Summary

A preliminary exploration of the performance and design spaces of the bulk and hybrid device architectures is performed to gain a better understanding of the capabilities of TECs. Subsequently, multiple single objective optimizations were explored to begin bridging the gap between theoretical, overarching conclusions and real world applications of TECs.

The incorporation of a cost metric that considers overall system costs and operating cost of a TEC allows a designer to work towards applications of the devices. Each of these optimizations offer a first pass analysis into the design of a TEC system, and the cost analysis provides a lower bound on the expected capital and operating costs of a TEC system. The information on the performance and design space is a significant resource on the hybrid and bulk architectures and their suitability to certain applications.

6. CONCLUSIONS AND FUTURE WORK

6.1. Summary of Thesis

Throughout this thesis, TEC potential for market application is explored using design optimization. Chapter 1 provided a brief overview of the principles behind thermoelectric devices, presents motivation for this work, and introduces the research questions. The primary motivation is to realize improved cooling and cost performance of TECs, as current capabilities of TE devices have not achieved the efficiency of current cooling technologies. While TECs might be a viable alternative to traditional vapor-compression refrigeration systems that employ potentially harmful refrigerants, the inefficiency of TECs has inhibited their adoption in more widespread applications. To address this limitation, two research goals are presented. The first was to determine what insights into the design and performance spaces of a TEC could be realized through design optimization and a new cost metric, and the second research question is aimed towards exploring future improvements to TECs that could be used to enhance their cooling and cost performance.

To understand the principles behind this work, Chapter 2 provided background information on thermoelectric materials, device architectures, roll-to-roll-processing, and previous design optimization, and Chapter 3 introduced the analytical model used to measure performance of the TEC system and introduces the cost metric used in this study. Towards investigating the research questions, the methodology presented in Chapter 4 introduces the optimization problems used in this study. Design parameters and properties were introduced to provide information to complete the analysis, and the optimization algorithms used to find the optimal solutions were described. While previous research has focused on solely the

trade-off between cooling capacity and device efficiency (*COP*), this study analyzed the trade-off between cooling capacity and system costs. Additional design variable considerations included material choices and heat exchanger characteristics. In addition to a multiobjective analysis, single objective problems were presented to further breakdown the operating and capital cost of the TECs to gain a deeper understanding of the device's economic characteristics. Lastly, Chapter 5 provides the results of the design optimization and discusses the insights gained and the potential for improvements in material efficiency and cost savings. The next section summarizes the findings from the results section to address the two research questions.

6.2. Addressing the Research Questions

In this section, the research questions aimed towards improving TECs to achieve wider adoption of its technology are revisited to summarize the findings of the results section and to discuss the conclusions of the work presented in this thesis.

Research question 1: What insights into the design and performance spaces of a thermoelectric cooler can be realized when using optimization and a new cost metric?

When selecting a TEC module, three parameters are needed to select a design: required cooling capacity, cold side temperature, and hot side temperature. While it is common throughout the literature to study optimal TECs and consider these three specifications, this study attempts to work towards real world applications by incorporating a cost metric and considering multiple facets of a TEC system, including heat exchangers and spreading resistance. Design optimization aimed at improving the performance of a TEC and a better understanding of TEC characteristics may allow for expanded use of TECs.

To achieve further insights into the design and performance spaces of a thermoelectric cooler, single and multiobjective optimization problems were presented. The design variables included leg length, leg width, leg thickness, spacing between the legs, input current, p-type thermoelectric material, n-type thermoelectric material, number of thermocouples, and the overall heat transfer coefficient of a heat exchanger. This study extended the work of other researchers by considering the multiobjective optimization of two different TEC architectures. To facilitate this optimization, the cost metric identified by Yee et. al is modified to accommodate the hybrid architecture and a heat exchanger on a thermoelectric cooler [42]. Optimization results allowed for comparisons between architectures while ensuring that the designs are evaluated for maximum cooling capacity and minimum cost. Results of the multiobjective optimization demonstrated the trade-off between cost and device performance. At different regions of the performance space, one device architecture or material choice may be a more appropriate solution for a given application. At high heat flux requirements, the bulk device with BiSbTe nanobulk material is the only option, but at lower heat flux requirements, both the hybrid and bulk devices are an option. However, the analysis suggests that the bulk device may still be the more economical alternative.

Like previous research, this analysis showed that maximizing leg area while decreasing leg length results in increased cooling capacities. Additionally, the BiSbTe nanobulk material is a promising alternative to the conventional BiTe modules currently on the market. Another design variable trend concluded in this study is the difference in optimal input current between the hybrid and bulk devices. As heat flux increases (i.e. more cooling

per unit area), the input current increases; as a result, the optimal current for the hybrid device was much lower than that for the bulk device. Another important takeaway from the results of this study is the impact of the heat exchanger on the design and performance of a TEC. Since the areas of the hybrid devices are very large, a heat exchanger with a lower heat transfer coefficient can be used to produce a cooling rate across the exchanger.

While these insights from the design optimization are important conclusions, TECs with current technologies still lag behind traditional methods of cooling in terms of efficiency. As mentioned previously, three areas of research exist to progress the advancement of TECs: improvements in thermoelectric materials, the use of design optimization, and the exploration of alternative device architecture [9]. The next research question addressed how future improvements in TE technology could address the limitations of TECs and how information on cost could offer insight into potential areas to investigate for economic advances in the design of a TEC.

Research question 2: How do improvements in the thermoelectric material figure of merit and identification of major cost components impact the performance outcomes of a thermoelectric cooler?

As the thermoelectric figure of merit (*ZT*) of a material increases, this directly translates into an increased *COP* of the TEC and thus reduced operating costs. Results presented in this work indicate that increasing *ZT* to around 3 resulted in *COP* values close to the Energy Star standard for central air conditioning standards [57]. With continued advancement of TE materials, the economic and cooling performance viability of TECs as an alternative to traditional cooling methods grows. However, after comparing results, it is

evident that even in low cooling density applications, the hybrid device architecture is not economically viable when compared to a bulk device. If printable TE materials can be improved to TE figure of merit (*ZT*) values similar to the material choices available for bulk devices, the hybrid architecture becomes a more attractive solution, as cost is less for a given cooling capacity than the bulk device. Like the bulk device though, further advancements in TE material technology are required to work beyond niche applications of TECs. The case study further demonstrates this while providing a relatable example of a TEC application, a compact refrigerator. With improvements in *ZT*, both the bulk and hybrid architectures become increasingly competitive alternatives to traditional vapor compression refrigeration.

Additionally, a majority of the total cost of a device is associated to operating cost, so consideration of the material efficiency and device *COP* is integral in the design of a TEC. These trends are similar in both the hybrid and bulk architectures. Capital cost, however, is still an important factor in designing a TEC. Heat exchangers are a large component of the TEC capital cost, particularly for the bulk device. The material cost is more expensive for the bulk device, but the large area of the hybrid device lends to a larger volume of material and substrate. In addition, the inexpensive polymer hybrid device is unable to compete from a performance standpoint with bulk devices and materials with higher *ZT* values. Consequently, the substrate and TE material are large components of the hybrid device's overall system cost, and even through the material is inexpensive, a sacrifice in performance exists to create deficiencies when compared to the bulk device. By identifying these major cost components, opportunities for savings and improvements are indicated.

6.3. Future Work

Future work includes an analysis of additional device architectures, including thin-film devices and a hybrid architecture with a sinusoidal structure. As identified through research question #2, it is evident that manufacturing constraints are limiting the performance of both the bulk and hybrid devices and that certain costs of heat exchanger, substrate, or material are prohibiting factors in the capital cost. While advancements in materials and manufacturing techniques are outside the scope of this research, further exploration of the limitations placed on the device architectures by currently available technology and of the available options for heat exchanger optimization is warranted. A detailed cost metric that comprehensively models the R2R manufacturing process for hybrid devices and the production of bulk TECs could contribute to a more complete understanding of these limitations. In addition, both R2R processing and device prototypes would provide further insights into the cost and cooling performance of the device architectures.

REFERENCES

[1] BCS, Incorporated, "Waste Heat Recovery: Technology and Opportunities in U.S. Industry." U.S. Departement of Energy.

[2] "Global Warming Potentials of ODS Substitutes | Ozone Layer Protection | US EPA." [Online]. Available: http://www.epa.gov/ozone/geninfo/gwps.html. [Accessed: 28-Jan-2015].

[3] D. M. Rowe, *Thermoelectrics handbook [electronic resource]□: macro to nano*. Boca Raton: CRC/Taylor & Francis, 2006.

[4] H. J. Goldsmid, *Introduction to Thermoelectricity*. Springer Science & Business Media, 2009.

[5] G. Chen, M. S. Dresselhaus, G. Dresselhaus, J.-P. Fleurial, and T. Caillat, "Recent developments in thermoelectric materials," *Int. Mater. Rev.*, vol. 48, no. 1, pp. 45–66, Feb. 2003.

[6] G. J. Snyder and E. S. Toberer, "Complex thermoelectric materials," *Nat. Mater.*, vol. 7, no. 2, pp. 105–114, Feb. 2008.

[7] R. I. A. C. (U.S.) and D. Nicholls, *System Reliability Toolkit*. RIAC, 2005.

[8] Ferrotec, "Thermal Reference Guide," *Ferrotec*. [Online]. Available: https://thermal.ferrotec.com/technology/thermal/thermoelectric-reference-guide/. [Accessed: 26-Jan-2014].

[9] L. E. Bell, "Cooling, Heating, Generating Power, and Recovering Waste Heat with Thermoelectric Systems," *Science*, vol. 321, no. 5895, pp. 1457–1461, Sep. 2008.

[10] F. J. DiSalvo, "Thermoelectric Cooling and Power Generation," *Science*, vol. 285, no. 5428, pp. 703–706, Jul. 1999.

[11] S. A. Abdul-Wahab, A. Elkamel, A. M. Al-Damkhi, I. A. Al-Habsi, H. S. Al-Rubai'ey', A. K. Al-Battashi, A. R. Al-Tamimi, K. H. Al-Mamari, and M. U. Chutani, "Design and experimental investigation of portable solar thermoelectric refrigerator," *Renew. Energy*, vol. 34, no. 1, pp. 30–34, Jan. 2009.

[12] "Advances In High-Performance Cooling For Electronics - Electronics Cooling Magazine - Focused on Thermal Management, TIMs, Fans, Heat Sinks, CFD Software, LEDs/Lighting," *Electronics Cooling Magazine - Focused on Thermal Management, TIMs, Fans, Heat Sinks, CFD Software, LEDs/Lighting*. .

[13] O. Bubnova, Z. U. Khan, A. Malti, S. Braun, M. Fahlman, M. Berggren, and X. Crispin, "Optimization of the thermoelectric figure of merit in the conducting polymer poly(3,4-ethylenedioxythiophene)," *Nat. Mater.*, vol. 10, no. 6, pp. 429–433, Jun. 2011.

[14] R. R. Søndergaard, M. Hösel, N. Espinosa, M. Jørgensen, and F. C. Krebs, "Practical evaluation of organic polymer thermoelectrics by large-area R2R processing on flexible substrates," *Energy Sci. Eng.*, vol. 1, no. 2, pp. 81–88, 2013.

[15] S. LeBlanc, S. K. Yee, M. L. Scullin, C. Dames, and K. E. Goodson, "Material and manufacturing cost considerations for thermoelectrics," *Renew. Sustain. Energy Rev.*, vol. 32, pp. 313–327, Apr. 2014.

[16] S. Song, V. Au, and K. P. Moran, "Constriction/spreading resistance model for electronics packaging," in *Proceedings of the 4th ASME/JSME thermal engineering joint conference*, 1995, vol. 4, pp. 199–206.

[17] K. Yazawa and A. Shakouri, "Scalable Cost/Performance Analysis for Thermoelectric Waste Heat Recovery Systems," *J. Electron. Mater.*, Jun. 2012.

[18] H. Kim, S.-G. Park, B. Jung, J. Hwang, and W. Kim, "New device architecture of a thermoelectric energy conversion for recovering low-quality heat," *Appl. Phys. A*, vol. 114, no. 4, pp. 1201–1208, Aug. 2013.

[19] Z. Lu, M. Layani, X. Zhao, L. P. Tan, T. Sun, S. Fan, Q. Yan, S. Magdassi, and H. H. Hng, "Fabrication of Flexible Thermoelectric Thin Film Devices by Inkjet Printing," *Small*, vol. 10, no. 17, pp. 3551–3554, Sep. 2014.

[20] Z. Cao, E. Koukharenko, M. J. Tudor, R. N. Torah, and S. P. Beeby, "Screen printed flexible Bi2Te3-Sb2Te3 based thermoelectric generator," *J. Phys. Conf. Ser.*, vol. 476, no. 1, p. 012031, Dec. 2013.

[21] A. Chen, D. Madan, P. K. Wright, and J. W. Evans, "Dispenser-printed planar thick-film thermoelectric energy generators," *J. Micromechanics Microengineering*, vol. 21, no. 10, p. 104006, Oct. 2011.

[22] A. Salleo and W. S. Wong, *Flexible electronics [electronic resource]□: materials and applications*. New York: Springer, c2009.

[23] C. B. Vining, "Semiconductors are cool," *Nature*, vol. 413, no. 6856, pp. 577–578, Oct. 2001.

[24] J.-C. Zheng, "Recent advances on thermoelectric materials," *Front. Phys. China*, vol. 3, no. 3, pp. 269–279, 2008.

[25] M. He, F. Qiu, and Z. Lin, “Towards high-performance polymer-based thermoelectric materials,” *Energy Environ. Sci.*, vol. 6, no. 5, pp. 1352–1361, Apr. 2013.

[26] H. Böttner, G. Chen, and R. Venkatasubramanian, “Aspects of Thin-Film Superlattice Thermoelectric Materials, Devices, and Applications,” *MRS Bull.*, vol. 31, no. 03, pp. 211–217, Mar. 2006.

[27] “Standard Modules,” *TE Technology, Inc.* [Online]. Available: https://tetech.com/peltier-thermoelectric-cooler-modules/standard/. [Accessed: 21-Feb-2015].

[28] T. Hendricks and W. T. Choate, “Engineering Scoping Study of Thermoelectric Generator Systems for Industrial Waste Heat Recovery,” U.S. Department of Energy, Nov. 2006.

[29] D.-J. Yao, G. Chen, and C.-J. Kim, “Design and Analysis of an In-Plane Thermoelectric Microcooler,” *Nanoscale Microscale Thermophys. Eng.*, vol. 14, no. 2, pp. 95–109, Apr. 2010.

[30] Q. Wei, M. Mukaida, K. Kirihara, Y. Naitoh, and T. Ishida, “Polymer thermoelectric modules screen-printed on paper,” *RSC Adv.*, vol. 4, no. 54, pp. 28802–28806, Jun. 2014.

[31] R. R. Søndergaard, M. Hösel, and F. C. Krebs, “Roll-to-Roll fabrication of large area functional organic materials,” *J. Polym. Sci. Part B Polym. Phys.*, vol. 51, no. 1, pp. 16–34, 2013.

[32] M. Yamanashi, “A new approach to optimum design in thermoelectric cooling systems,” *J. Appl. Phys.*, vol. 80, no. 9, pp. 5494–5502, Nov. 1996.

[33] B. J. Huang, C. J. Chin, and C. L. Duang, “A design method of thermoelectric cooler,” *Int. J. Refrig.*, vol. 23, no. 3, pp. 208–218, May 2000.

[34] Y. Zhou and J. Yu, “Design optimization of thermoelectric cooling systems for applications in electronic devices,” *Int. J. Refrig.-Rev. Int. Froid*, vol. 35, no. 4, pp. 1139–1144, Jun. 2012.

[35] Y.-X. Huang, X.-D. Wang, C.-H. Cheng, and D. T.-W. Lin, “Geometry optimization of thermoelectric coolers using simplified conjugate-gradient method,” *Energy*, vol. 59, pp. 689–697, Sep. 2013.

[36] Y.-H. Cheng and W.-K. Lin, “Geometric optimization of thermoelectric coolers in a confined volume using genetic algorithms,” *Appl. Therm. Eng.*, vol. 25, no. 17–18, pp. 2983–2997, Dec. 2005.

[37] Y.-H. Cheng and C. Shih, “Maximizing the cooling capacity and COP of two-stage thermoelectric coolers through genetic algorithm,” *Appl. Therm. Eng.*, vol. 26, no. 8–9, pp. 937–947, Jun. 2006.

[38] P. K. S. Nain, J. M. Giri, S. Sharma, and K. Deb, “Multi-objective Performance Optimization of Thermo-Electric Coolers Using Dimensional Structural Parameters,” in *Swarm, Evolutionary, and Memetic Computing*, vol. 6466, B. K. Panigrahi, S. Das, P. N. Suganthan, and S. S. Dash, Eds. Berlin: Springer-Verlag Berlin, 2010, pp. 607–614.

[39] D. V. K. Khanh, P. Vasant, I. Elamvazuthi, and V. N. Dieu, “Optimization Of Thermo-Electric Coolers Using Hybrid Genetic Algorithm And Simulated Annealing,” *Arch. Control Sci.*, vol. 24, no. 2, pp. 155–176, 2014.

[40] R. Venkata Rao and V. Patel, “Multi-objective optimization of two stage thermoelectric cooler using a modified teaching–learning-based optimization algorithm,” *Eng. Appl. Artif. Intell.*, vol. 26, no. 1, pp. 430–445, Jan. 2013.

[41] B. Abramzon, “Numerical Optimization of the Thermoelectric Cooling Devices,” *J. Electron. Packag.*, vol. 129, no. 3, pp. 339–347, Nov. 2006.

[42] S. K. Yee, S. LeBlanc, K. E. Goodson, and C. Dames, “$ per W metrics for thermoelectric power generation: beyond ZT,” *Energy Environ. Sci.*, vol. 6, no. 9, pp. 2561–2571, Aug. 2013.

[43] H. Kim and W. Kim, “A way of achieving a low $/W and a decent power output from a thermoelectric device,” *Appl. Energy*, vol. 139, pp. 205–211, Feb. 2015.

[44] “RotaMesh Specifications,” *SPGPrints Am. Inc*, no. rev.10.10a.

[45] P. Yates, “Quote Request from spgprints.com,” 12-Nov-2014.

[46] H. Lee, “The Thomson effect and the ideal equation on thermoelectric coolers,” *Energy*, vol. 56, pp. 61–69, Jul. 2013.

[47] R. K. Shah and D. P. Sekulic, *Fundamentals of Heat Exchanger Design*. John Wiley & Sons, 2003.

[48] L. M. Matthews, *Estimating manufacturing costs□: a practical guide for managers and estimators /*. McGraw-Hill, c1983.

[49] “National Minerals Information Center,” *Minerals Statistics and Information from the USGS*. .

[50] R. Hankey, C. Cassar, R. Peterson, P. Wong, and J. Knaub, Jr., “Electric Power Monthly with Data for October 2014,” U.S. Department of Energy, Washington, DC, Dec. 2014.

[51] F. Esposito, “Resin Pricing,” *Plastics News*, 12-Jan-2015. [Online]. Available: http://www.plasticsnews.com/resin/engineering-thermoplastics/current-pricing.

[52] P. Auerkari, “Mechanical and physical properties of engineering alumina ceramics,” 1996.

[53] J. Speight, *Lange’s Handbook of Chemistry, 70th Anniversary Edition*. McGraw-Hill Companies,Incorporated, 2004.

[54] K. Deb, A. Pratap, S. Agarwal, and T. Meyarivan, “A fast and elitist multiobjective genetic algorithm: NSGA-II,” *IEEE Trans. Evol. Comput.*, vol. 6, no. 2, pp. 182–197, Apr. 2002.

[55] “Global Optimization Toolbox: User’s Guide (R2013b).” The MathWorks, Inc., 2004.

[56] S. Kirkpatrick, M. P. Vecchi, and others, “Optimization by simmulated annealing,” *science*, vol. 220, no. 4598, pp. 671–680, 1983.

[57] “Air-Source Heat Pumps and Central Air Conditioners Key Product Criteria,” *Energy Star*, 19-Jan-2015. [Online]. Available: https://www.energystar.gov.

[58] R. Ranjan, J. E. Turney, C. E. Lents, and V. H. Faustino, “Design of Thermoelectric Modules for High Heat Flux Cooling,” *J. Electron. Packag.*, vol. 136, no. 4, p. 041001, Dec. 2014.

[59] “Window Air Conditioners Heat/Cool,” *LG Electron. USA Inc*, Nov. 2013.

[60] “Frigidaire 2.4 Cu. Ft. Compact Refrigerator Black - FFPE2411QB.” [Online]. Available: http://www.frigidaire.com/Kitchen-Appliances/Refrigerators/Compact-Refrigerator/FFPE2411QB/. [Accessed: 09-Mar-2015].

[61] *Winco SPFD2 2-1/2-Inch Divider Food Pan, Full Size*. .

[62] O. of the Commissioner, “Consumer Updates - Are You Storing Food Safely?” [Online]. Available: http://www.fda.gov/ForConsumers/ConsumerUpdates/ucm093704.htm. [Accessed: 09-Mar-2015].